FATIGUE RESISTANCE OF HOT-MIX ASPHALT CONCRETE (HMAC)

MIXTURES USING THE CALIBRATED MECHANISTIC WITH SURFACE

ENERGY (CMSE) MEASUREMENTS APPROACH

A Thesis

by

EDWARD KWAME OFORI-ABEBRESSE

Submitted to the Office of Graduate Studies of
Texas A&M University
in partial fulfillment of the requirements for the degree of

MASTER OF SCIENCE

August 2006

Major Subject: Civil Engineering

FATIGUE RESISTANCE OF HOT-MIX ASPHALT CONCRETE (HMAC)

MIXTURES USING THE CALIBRATED MECHANISTIC WITH SURFACE

ENERGY (CMSE) MEASUREMENTS APPROACH

A Thesis

by

EDWARD KWAME OFORI-ABEBRESSE

Submitted to the Office of Graduate Studies of
Texas A&M University
in partial fulfillment of the requirements for the degree of

MASTER OF SCIENCE

Approved by:

Co-Chairs of Committee,	Amy Epps Martin
	Charles Glover
Committee Member,	Dallas N. Little
Head of Department,	David Rosowsky

August 2006

Major Subject: Civil Engineering

ABSTRACT

Fatigue Resistance of Hot-Mix Asphalt Concrete (HMAC) Mixtures Using the Calibrated

Mechanistic with Surface Energy (CMSE) Measurements Approach. (August 2006)

Edward Kwame Ofori-Abebresse, B.Sc., KNUST, Ghana

Co-Chairs of Advisory Committee: Dr. Amy Epps Martin
                                                          Dr. Charles Glover

Fatigue cracking is one of the fundamental distresses that occur in the life of a

Hot Mix Asphalt Concrete (HMAC) pavement. This load induced distress leads to

structural collapse of the entire pavement ultimately and can only be remedied by

rehabilitation. There is the need, therefore, for a total understanding of the phenomenon

to be able to counter its occurrence. The fatigue resistance of hot mix asphalt concrete

(HMAC) has been estimated using approaches ranging from empirical methods to

mechanistic-empirical methods to purely mechanistic methods. A continuum mechanics

based approach called the Calibrated Mechanistic with Surface Energy (CMSE)

measurements was developed at Texas A&M University and recommended after

comparison with other approaches in predicting fatigue lives of two Texas HMAC

mixtures. The CMSE approach which includes fundamental material properties such as

fracture, aging, healing, and anisotropy has been shown to effectively model the

parameters that affect the performance of HMAC pavements exposed to repetitive traffic

loads.

Polymer modified asphalt (PMA) improves pavement performance by providing

additional resistance to the primary distresses in flexible pavements, including permanent

deformation or rutting, thermal cracking, and fatigue cracking. In this research, the CMSE approach was utilized to estimate the fatigue resistance of HMAC fabricated with asphalts modified with Styrene-butadiene-Styrene (SBS) co-block polymer. These HMAC mixtures were fabricated from materials used on three different road sections in Texas and one test pavement in Minnesota.

The CMSE approach was validated as an effective approach for estimating the fatigue resistance of HMAC mixtures with PMA. The effect of oxidative aging on the fatigue resistance of the HMAC mixtures was also verified. Oxidative aging of the mixtures resulted in a corresponding decrease in mixture fatigue resistance. In addition, for two HMAC mixtures with the same binder content and aggregate gradation, the mixture with the softer of the two Performance Grade (PG) binders exhibited greater fatigue resistance. The use of the Utility Theory revealed the possible effects of aggregate geometric properties on the HMAC mixture properties and consequently on their fatigue resistance.

DEDICATION

This thesis is dedicated to my family, especially my mother Adwoa Abebresse and my kid brother Emmanuel Kwesi Abedi Abebresse.

ACKNOWLEDGEMENTS

TABLE OF CONTENTS

TABLE OF CONTENTS (continued)

TABLE OF CONTENTS (continued)

LIST OF FIGURES

LIST OF FIGURES (continued)

LIST OF TABLES

LIST OF TABLES (continued)

CHAPTER I

INTRODUCTION

PROBLEM STATEMENT

As of 2001 in the United States, there were 2.5 million miles of flexible pavements (Huang 2004). Several distresses hamper the performance of these pavements and result in premature failure. In flexible pavements, the primary forms of distress are fatigue cracking, rutting, and thermal cracking. These distresses manifest themselves most of the time due to construction material quality, poor maintenance, and improper design. A complete description of the distresses and failure mechanisms is described in The Highway Pavement Distress Identification Manual (Smith et al. 1979).

Rutting develops in the early life of a flexible pavement and is caused by a combination of consolidation and shear deformation in the pavement layers. At high temperatures, the Hot Mix Asphalt Concrete (HMAC) layer is less stiff and thus flows.

Upon the application of traffic loads, there is densification of the layer that leaves a depressed surface in the wheel paths as evidence of rutting. In other cases, inadequate compaction and stiffness of the supporting pavement layers causes consolidation of these layers which then leads to ultimate settling of the HMAC layer which also shows as depressed surfaces known as rutting.

This thesis follows the style of *Journal of Materials in Civil Engineering (ASCE).*

At low temperatures, the stiffness of HMAC increases and cracks develop due to its brittle nature and the reduction in temperatures that leads to restrained shrinkage of the HMAC and induced thermal stresses. This form of distress is known as thermal cracking, and the distress manifests itself as regularly spaced transverse cracks.

Fatigue cracking is the third primary form of distress in flexible pavements. This type of distress occurs at intermediate temperatures under repetitive traffic loading. It occurs over the long term, but once it initiates it progresses rapidly and leads to a total structural collapse of the pavement. This distress is commonly referred to as alligator cracking because its pattern resembles the skin of an alligator.

To prevent the development of rutting which develops in the early life of the pavement, researchers and pavement engineers have resorted to increasing the stiffness of the HMAC layer at high temperatures. It is assumed that once this is done the HMAC will not flow and rut in the early life of the pavement. Some of the mechanisms that have been adapted to increase HMAC stiffness include polymer modification. This has worked well and drastically reduced the number of pavements that fail due to rutting. However, the high stiffness of the HMAC makes it brittle and therefore susceptible to cracking under repeated traffic loading. Therefore though rutting in the pavements is prevented, the problem of fatigue cracking remains.

Current research is focused on increasing the fatigue resistance of HMAC. Again, some of the methods suggested include polymer modification. Even though the stiffness of the HMAC is increased and therefore made brittle, other inherent properties in the polymer modified asphalts make the mixture resistant to fatigue cracking. The question remains as to what extent do the fatigue resistant properties in the polymer modified

HMAC compensate for the brittleness created as a result of increased stiffness of the HMAC.

In addition to the polymer modified asphalt (PMA), the aggregate in HMAC mixtures also contributes to mixture resistance to fatigue cracking. Aggregates form 85% of the volume of HMAC and provide the structure that resists applied traffic load. The role of aggregates in the resistance of pavement distresses has been studied extensively, but most efforts concentrated on the role of aggregates in resisting permanent deformation and improving skid resistance (Mahmoud 2005). Aggregates may also play an effective role in the resistance of fatigue cracking Dense graded, open-graded, gap graded, and many other Superpave and State Department of Transportation's aggregate gradations or structures have been used in HMAC mix designs. They have been used as a means of resisting different distresses and improving permeability of the HMAC. The question remains as to which of these aggregate structures performs better in fatigue resistance and what properties of the aggregate are needed to facilitate effective resistance to repetitive load applications?

Geometric properties of aggregates have been measured and correlated to the performance of HMAC mixtures (Fletcher et al. 2003). The aggregate geometric properties measured with high a level of accuracy using imaging techniques include shape, angularity, and texture. These measurements facilitate exploration of the influence of aggregate properties on the long term performance of HMAC.

Several methods used in predicting the fatigue resistance of HMAC have been proposed and used. These have been empirical and mechanistic in nature. The Asphalt Institute model and the Shell nomograph are among the early empirical models that have

been used. Another common mechanistic-empirical approach which has been used extensively is the bending beam flexural fatigue test. Some mechanistic models incorporating the use of fracture mechanics, dissipated energy, and other concepts which have sought to predict fatigue resistance based on the fundamental behavior of crack initiation and propagation in the HMAC have also been proposed and used. The Calibrated Mechanistic with Surface Energy (CMSE) measurements is one of the these mechanistic approaches in use today. This approach predicts fatigue resistance based on the material properties of the HMAC mixture and component materials. In a separate study comparing this approach with other fatigue prediction approaches, the CMSE produced fatigue lives with the lowest variability (Walubita 2006).

RESEARCH OBJECTIVES

Based on the introduction, the following objectives are proposed for this research:

- To validate the CMSE approach as a reliable tool to measure the fatigue resistance of selected HMAC mixtures.
- To evaluate and compare the fatigue resistance of selected HMAC mixtures that vary in terms of mixture type, aggregate geometric properties, and binder type.
- To evaluate and quantify the influence of other factors such as aggregate geometric properties on the fatigue resistance of the selected HMAC mixtures.

SCOPE OF STUDY

The scope of this research will be limited to the following:

- Six HMAC mixtures: two being studied in the Minnesota Department of Transportation (MnDOT) MnROAD Research study and four Texas Department of Transportation (TxDOT) mixtures used in the Atlanta, Odessa, and Waco Districts.

- Five different aggregate types: gravel, igneous, rhyolite, quartzite, and sandstone used in the six HMAC mixtures.

- Three aggregate structures: Superpave 12.5mm, Superpave 19mm, and a Coarse Matrix High Binder type F (CHMB_F) used in Texas.

- Four polymer modified asphalts (PMA) utilizing SBS co-block polymer: PG 76-22, PG 70-22, PG 58-34, and PG 58-40.

- Three mixture oxidative aging conditions that simulate Texas HMAC field aging: 0, 3, and 6 months aging in a 60°C environmental room.

- One fatigue analysis approach: the CMSE recommended in TxDOT Project 0-4468.

- One Aggregate Imaging Measurement System (AIMS) used by the International Center for Aggregate Research (ICAR) for the measurement of aggregate shape and texture.

THESIS LAYOUT

This thesis is organized in six chapters. Chapter I is an introductory chapter outlining the problem statement and the objectives for the research. The scope of the study is clearly stated in this chapter as well as a layout of the thesis. A summary of the chapter is then provided at the end.

Chapter II focuses on an extensive literature review beginning with an introduction. An overview is given of the different approaches employed to characterize HMAC mixtures in terms of fatigue resistance. The effects of PMA in HMAC mixture fatigue resistance is explored, as well as the influence of aggregate geometric properties. A summary is also given at the end of this chapter.

The research methodology is the main theme in Chapter III. The experimental design for the HMAC is given with the material properties for the binders and aggregates. The methodology used in the HMAC mixture fabrication is outlined, and the analytical measurements used to characterize the mixtures in terms of fatigue resistance are also discussed. The analysis procedure employed in the CMSE is explained, and a summary of the chapter is provided at the end.

Chapter IV describes the laboratory test results. In this chapter the test results from the aggregate characterization, surface energy tests of the asphalts and aggregates, as well as the results of the HMAC CMSE tests are provided. As with the other chapters, a summary is also provided at the end of this chapter.

The discussion of the results presented in Chapter IV is given in Chapter V. This chapter contains the discussion of the predicted fatigue resistance of the HMAC mixtures and an evaluation of the effects of aggregate geometric properties on the fatigue resistance of the mixtures. A summary of the discussion is given at the end of the chapter.

Chapter VI includes a list of conclusions and recommendations from this study.

SUMMARY

This chapter provides an introduction to the research proposed for this thesis. In the problem statement, a summary is given about the various distresses in flexible pavements with an emphasis on fatigue cracking. The research objectives and the scope of study are also outlined, and the organization of the thesis completes the chapter.

CHAPTER II

LITERATURE REVIEW

INTRODUCTION

Flexible pavements are layered structures with HMAC surfacing, and they typically bend or deflect when subjected to traffic loads. Materials of higher quality or stiffness generally lie on top of layers with lower quality materials. Because flexible pavements are common in the United States (U.S.), extending their life by resisting distress is of interest to researchers and pavement engineers. One primary form of distress is fatigue cracking, which is a long term distress mode that has not been given extensive study as compared to rutting or permanent deformation. This is due to the fact that fatigue cracking occurs in the later stages of a pavement's life. However, this distress mode constitutes a structural failure, and once it begins the safety of the pavement is compromised.

This literature review is composed of four sections that examine this failure mechanism from different perspectives. The different approaches that have been used to measure the fatigue resistance of HMAC will be outlined, as well as the effects of polymer modification of asphalts as a means of improving the fatigue resistance of HMAC. The role of aggregates in the fatigue resistance of HMAC will also be evaluated, and then a summary of the salient points in the literature review will be provided at the end of the chapter.

FATIGUE RESISTANCE IN HOT MIX ASPHALT CONCRETE

A flexible pavement structure consists of different layers, typically an HMAC surface layer, a granular base layer, and an optional subbase layer, and the underlying subgrade. To ensure effective performance, the materials used in the different layers should be of high quality and of a stiffness level commensurate with the loads anticipated during the life of the pavement. A flexible pavement fails in fatigue due to repeated load applications which induce stresses beyond what the structure can sustain. Inadequate drainage in the underlying layers could cause them to be saturated with water and thus lose their strength. When this happens the strength bearing capacity of the structure is reduced and the HMAC layer alone is not able to sustain the traffic loads and fails in fatigue. In other cases, poor material quality during construction makes the structure weak and unable to sustain loads for which they were designed and causes failure in fatigue.

The predominant material property governing the fatigue failure mechanism is the tensile strain in the HMAC layer. Once the induced tensile strain due to the applied loads exceed the design tensile strain of the pavement, fatigue cracking initiates and eventually leads to failure of the structure. Common rehabilitation measures adopted to offset this distress are removal and replacement of the entire layer that causes the failure or the use of overlays.

Two modes of failure govern fatigue cracking failure in flexible pavements. These are top-down fatigue cracking and bottom-up fatigue cracking. A pictorial representation of these two failure modes of fatigue cracking is shown in Figure 2.1. Bottom-up cracking is primarily caused by high tensile stresses at the bottom of the HMAC layer.

This could be due to inadequate stiffness of the base or the HMAC layer. When the tensile strain induced by traffic loads exceeds that which the HMAC layer can sustain, a mode I crack failure occurs. The crack initiates at the bottom of the layer and with continuous repeated traffic load application propagates to the top of the layer. Top down fatigue cracking, however, is associated with mode II cracking. The crack initiates from the top of the pavement and propagates downwards through the pavement structure. The shearing action of the traffic loads induce shear strains and when the induced strain exceed the design level for the pavement, the cracks initiate. Aging of HMAC increases stiffness and results in brittleness. The brittle nature of the aged HMAC cause crack initiation with the application of traffic loads.
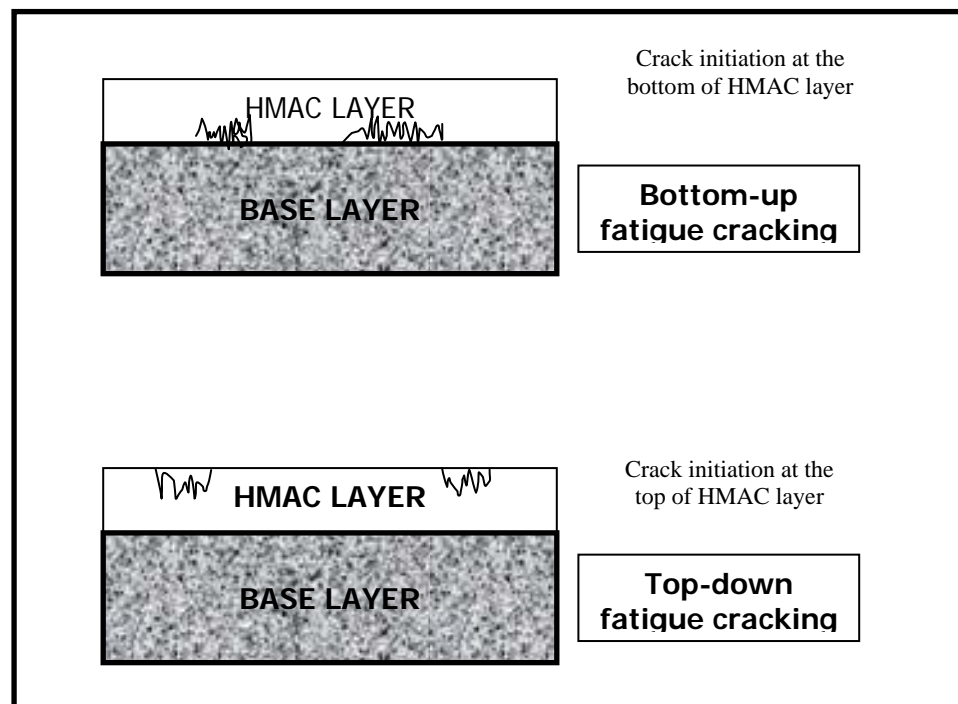
Figure 2.1 Failure Modes Governing Fatigue Cracking

Whichever the fatigue cracking failure mode, the resistance of HMAC to fatigue cracking failure can be predicted by a number of different approaches. Walubita (2006) compared four different approaches, including the Mechanistic-Empirical (ME), the Calibrated Mechanistic with and without Surface Energy (CMSE/CM) measurements, and the proposed National Cooperative Highway Research Program (NCHRP) 1-37A Mechanistic Empirical Pavement Design Guide (MEPDG).

In the ME approach, HMAC beams are compacted with the Linear Kneading Compactor. The kneading compaction was selected to represent field compaction of HMAC. The beams are subjected to repeated sinusoidal loading under a controlled strain mode, and an empirical fatigue relationship is determined. A hypothetical pavement structure is then used in a structural linear elastic model to determine the critical strain that will develop at the bottom of the HMAC pavement under traffic loading. The empirical fatigue relationship is then used to predict laboratory fatigue life of the HMAC, and then various shift factors are applied to this prediction to account for interactions in the field that cannot be simulated or accounted for in the laboratory testing protocol. Some of the shift factors employed in the ME protocol account for temperature, traffic wander, construction variability, loading frequency, crack propagation and healing. A reliability multiplier was applied to the laboratory fatigue life, and then a check is made as to the adequacy of the fatigue resistance of the HMAC in a specific pavement structure if laboratory fatigue life multiplied by a reliability factor exceeds the traffic anticipated under field conditions. This model only considers one of the failure modes, bottom-up cracking.

The NCHRP 1-37A's proposed MEPDG was also explored. In this approach, asphalt binder Dynamic Shear Rheometer (DSR) tests are conducted using the AASHTO PP1 test protocol and the Dynamic Modulus (DM) test is conducted on cylindrical HMAC specimens over a range of temperatures and frequencies using the AASHTO (2003) TP 62-03 protocol. The Complex Shear Modulus (G*) of the binder and the Dynamic Modulus (E*) of the mixture from these two tests were inputs in the MEPDG software. The percentage cracking in the wheel paths of the input pavement structure is determined, and statistical applications are used to predict fatigue lives corresponding to 50% cracking in the wheel paths. This method considers both failure modes of fatigue cracking, top-down and bottom-up.

To address the limitations of the mechanistic empirical approaches, a calibrated mechanistic approach incorporating the use of fracture mechanics and continuum mechanics is also utilized. The two mechanistic approaches employed are the Calibrated Mechanistic with (CMSE) and without (CM) Surface Energy measurements. In both approaches, HMAC cylindrical specimens are tested in strength, relaxation, and repeated load tests in uniaxial tension and compression. In this method, the bond strength for the HMAC is determined using surface energy components of the asphalt binder and the aggregates measured separately.

The CMSE approach was found to be the best of the four approaches considering many factors outlined in Table 2.1. This approach was thus recommended for use in this research. Details of the approach together with testing equipment and analysis are described in Chapter III of this thesis.

Table 2 .1 Comparison of Fatigue Analysis Approaches (After Walubita 2006)

Item	Fatigue Analysis Approaches		
	MEPDG	**ME**	**CMSE/CM**
Concept	Mechanistic-Empirical based	Mechanistic-Empirical based	Continuum Mechanics and HMAC fundamental properties
Lab Testing	Easy but lengthy temperature conditioning time	Rigorous and lengthy	Numerous but easy to run and less costly
Testing Time	$\cong$ 5hrs	$\cong$ 30hrs	$\cong$ 70 hrs
Equipment cost	$\cong$ $130,000 excluding the cost of software	$\cong$ $155,000 ($\cong$ 25,560 for the Bending Beam device	$\cong$ $210,000
Input Data	Comprehensive/flexible	Comparatively few	Comprehensive
COV of Input Data	$\cong$ 5 - 23%	$\cong$ 5 – 28%	$\cong$ 4 – 12%
Failure Criteria	50% cracking in wheel path	50% reduction in flexural stiffness	7.5mm micro crack growth through the HMAC layer thickness
Analysis Procedure	Comprehensive but its software based	Relatively easy and straightforward	Comprehensive and lengthy
Analysis time	$\cong$ 4.5hrs	$\cong$ 3hrs	$\cong$ 6hrs (5hrs for CM)
Failure Load response parameter	Maximum critical design tensile strain @ bottom of HMAC layer	Maximum critical design tensile strain @ bottom of HMAC layer	Maximum critical design shear strain @ edge of loaded tire

EFFECTS OF POLYMER MODIFIED ASPHALT (PMA) ON HMAC MIXTURE FATIGUE PERFORMANCE

PMAs have been successfully used to reduce the incidence of several HMAC pavement distresses; moisture damage, permanent deformation, and thermal fatigue

cracking (Williamson and Gaughan 1992; Othman et al. 1995; Khattak and Baladi 1998; Goulias D. G., 2001). Fatigue cracking is a long term pavement load associated distress which eventually leads to structural collapse of the HMAC pavement. Over concentration on the early pavement distresses seem to have overshadowed the quest to attain fatigue resistant HMAC pavements. Increase in vehicle ownership leading to increased traffic volumes across the US in recent years calls for concern to this distress as this will eventually lead to shortened HMAC pavement life through fatigue cracking. In this section, the effect of PMA in fatigue resistance of HMAC will be discussed.

Use of PMAs in HMAC Pavements

Polymer Modified Asphalts (PMA) are products obtained from the chemical combination of thermoplastic elastommers and plastomers with base asphalts to form products that have enhanced properties and thus superior performance (Brule 1996). Styrene-butadiene-styrene (SBS) and tire rubber are the two modifiers that have gained currency in recent years owing to their superior performance in HMAC. PMAs have enhanced properties compared to traditional unmodified asphalts. PMAs have low susceptibility to temperature and loading time, and this increases their resistance to permanent deformation and fatigue cracking (Brule 1996). To date PMAs have become an important component in HMAC, and on-going research seeks to improve the understanding of these materials and their performance in HMAC pavements.

Properties of PMAs That Enhance Resistance to Fatigue Cracking

Improvement in the performance of HMAC that contain PMAs is largely due to the improvement in the rheological properties of the binders. The rheological properties of a binder that allow flexibility under load controls resistance to fatigue. To adequately

resist fatigue cracking, HMAC should be able to withstand tensile strains induced from traffic loads. Polymer modification increases the viscosity of the asphalt binder, and this increase in viscosity causes a corresponding increase in tensile and compressive strengths of the HMAC (Khattak and Baladi 2001). Fatigue is induced by tension, and thus an improvement in the tensile strength property of the mix is seen as improvement in fatigue resistance. Improved binder-aggregate adhesion and the formation of a strong polymer network structure are additional reasons for the improvement in tensile and compressive strengths of polymer modified HMAC (Khattak and Baladi 2001). Statistical models produced using a range of PMAs showed a strong correlation between rheological properties of PMAs and engineering properties (tensile and compressive strength) of the PMA mixtures (Khattak and Baladi 2001).

Fatigue cracking is a long term pavement distress, and as the pavement ages the binder is oxidized and it becomes stiffer. As a result of this increased stiffness, large shear stresses induced due to increased tire pressures also induce top-down fatigue cracking. Aging associated with oxidation in the HMAC causes an increase in viscosity and makes the HMAC susceptible to disintegration, cracking, and moisture susceptibility (Bell 1990). PMAs improve the aging susceptibility of HMAC. They performed better in terms of field aging resistance compared to mixtures with conventional asphalt binders (Lufti et al. 2001).

Fracture toughness is an important property that aids resistance to fracture damage of materials. Increased fracture toughness is achieved by the use of PMAs in HMAC. An increase in the percentage of the modifiers used in the PMA increased the fracture toughness, but for reasons of workability and cost, the percentage of modifiers

has remained stable from 3 – 6% by weight of the base asphalt (Aglan et al. 1993; Kuennen 2005). In a related research study scanning electron microscope images revealed better binder-aggregate adhesion with the use of PMAs, and this was shown to increase the toughness of the HMAC fabricated with PMAs (Aglan et al. 1993).

Future Research on the Use of PMA for Fatigue Resistance

PMAs are steadily increasing in their use in the road construction industry. However, more research work is needed. In addition to increasing stiffness, PMAs also affect workability (Kuennen 2005). This means that mixing and compaction operations need to be properly timed to enable adequate compaction to be achieved in the field. A new protocol needs to be developed to look at the mixing and compaction temperatures for PMA HMAC. The Superpave parameters were also developed for conventional asphalts but have been used to grade PMAs. The Superpave fatigue parameter, specifically, needs re-evaluation for PMAs (Dongre et al. 1997). Binder compatibility is also another concern. Some modifiers react differently depending on the base binder that is used. In a recent study, the addition of modifiers to an AC – 30 asphalt produced a PMA which was brittle with age whereas with other base asphalts it was softer with age (Huang et al. 1995). The major disincentive to the use of PMAs is a cost increase from 30 to 100% compared to conventional asphalts and an ultimate cost increase of 10 to 40% for the corresponding HMAC (Kuennen 2005).

AGGREGATE CHARACTERIZATION FOR HMAC AND ITS EFFECT ON FATIGUE RESISTANCE

HMAC is comprised of aggregate, asphalt, and air with the aggregates making up about 85% of the total volume. Thus aggregates play a significant role in HMAC performance. Many studies on the role of aggregates in resisting the primary distresses that occur in flexible pavements have been done (Epps and Monismith 1972; Huang and Grisham 1972; Karakouzian et al. 1996; Chen and Liao 2002). In particular, the aggregate structure in terms of the gradation plays an important role in determining the resistance of mixtures to the primary distresses in flexible pavements.

Since aggregates play such a vital role in the properties of the HMAC, it is necessary to quantify the properties which aid the resistance to distress so that aggregates of the best quality will be selected for paving projects. In a study on rutting for example, HMAC resisted this distress adequately if a sufficient range of particles passing sieve size number 4 (4.75mm) is specified (Chen and Liao 2002). In another study also on rutting, 50% rutting reduction was achieved when both coarse graded and skip graded aggregates were used instead of the conventional continuous graded aggregates (Karakouzian et al. 1996). These two studies highlight that when the consensus properties of aggregate and their structure are studied effectively, specification of aggregate properties and structure that will adequately resist the distress is possible.

The study of aggregates and their effect on distress has concentrated on rutting, and little work has been done on fatigue. This primarily can be attributed to the fact that rutting occurs in the early life of a pavement and this is of immediate concern. However, there remains a need to look at the role aggregates play in the resistance to fatigue.

Conflicting results have been obtained in studies of this nature. In a review of fatigue in asphalt concrete mixtures, asphalt content and test temperature appeared to be more critical than the variation of aggregate gradation in the resistance to fatigue cracking (Epps and Monismith 1972). In a similar circumstance, the fatigue behavior of HMAC mixtures was found to be insensitive to the geometric characteristics of coarse aggregates and their gradation (Huang and Grisham 1972). The fatigue lives of HMAC mixtures were found to increase with the particle index of the fine aggregates (Huang and Grisham 1972).

It is well known that air voids content have a significant effect on the fatigue lives of HMAC. To achieve optimum air voids, the aggregate shape, texture, and angularity have to be carefully considered. The amount of asphalt that can be absorbed in a mix is dependent on the surface texture of the mix. Rough surface textured aggregates provide good bonding between the asphalt and the aggregates, and such good adhesion is necessary for fatigue resistance. The compatibility of the mix is also dependent on the aggregate shape and angularity. With adequate researched, specifications to produce a high quality paving material adequate to resist fatigue cracking will be possible. In fact, Analysis of Variance (ANOVA) of some HMAC mixture tests revealed that aggregates with rough surface texture and angular shape showed better fatigue performance (Kim et al. 1992).

The stiffness of an HMAC mixture is critical for its fatigue resistance, and the contributions of aggregate type, aggregate gradation and air void content on mixture stiffness are shown in Table 2.2.

Table 2.2 Factors Affecting the Stiffness of HMAC (after Monismith 1970)

Factor	Change in Factor	On stiffness
Aggregate Type	increase roughness and angularity	increase
Aggregate Gradation	open to dense gradation	Increase
Air Void Content	decrease	Increase

Aggregate characterization has increased in popularity recently. The Superpave methods have been fraught with inconsistencies. The restricted zone for instance has been found insufficient to characterize aggregate gradation to ensure acceptable rutting performance (Hand et al. 2001). The Superpave methods for characterizing aggregate shape, texture, and form have also been found to be imprecise (Fletcher et al. 2003). With the advancement in technology, aggregates are now being characterized using computer automated image analysis. The University of Illinois Aggregate Image Analyzer and the Aggregate Imaging System (AIMS) have both been used to measure aggregate characteristics, and a strong correlation has been found with performance in HMAC (Fletcher et al. 2003; Pan and Tutumluer 2005). In the use of these image analysis tools to measure the 3-dimensional form of aggregates, a good correlation was found between the measurements and those done directly with digital calipers (Fletcher et al. 2003). It therefore remains to find out the role the aggregate surface texture, angularity, and form play in the fatigue resistances of HMAC mixtures.

SUMMARY

This chapter represents the literature review associated with this research. A review of fatigue approaches by Walubita (2006) is presented. The effect of PMA on fatigue cracking in HMAC is also discussed, as well as the role of aggregate characteristics in HMAC fatigue resistance.

CHAPTER III

RESEARCH METHODOLOGY

INTRODUCTION

In this research the CMSE approach for determination of fatigue resistance was used. AIMS used by the International Centre for Aggregate Research (ICAR) was also applied to measure the aggregate shape and texture characteristics of the aggregates used in the HMAC mixtures. This chapter looks extensively at the methodology adopted for the study. The experimental design for the HMAC mixtures, the HMAC specimen fabrication, the hypothetical pavement structure used for comparison together with the environmental conditions, the analytical measurements, the analysis procedure and a summary of the chapter is provided.

EXPERIMENTAL DESIGN

In this study, six different HMAC mixtures were studied. These mixtures were those used in three Texas Department of Transportation (TxDOT) Districts: Atlanta, Waco, and Odessa and a test pavement section in Minnesota. These HMAC mixtures contained five different aggregate types: gravel, igneous, rhyolite, sandstone, and quartzite with five different gradations and four PMAs.

The HMAC mixtures will be referred to as MnROAD 01, MnROAD 02, Waco, Odessa, Atlanta Sandstone, and Atlanta Quartzite. The description of these mixtures

follows in the next section. Table 3.1 presents a summary of the mixture matrix used in this experimental design.

Table 3.1 HMAC Mixture Matrix

Mixture	Aggregate	Asphalt	Mix Type	Asphalt Content by weight of mixture (%)
MnROAD 01	Gravel	PG 58-34	Superpave 12.5mm	5.8
MnROAD 02		PG 58-40		
Waco	Igneous		Superpave 19mm	5.3
Odessa	Rhyolite	PG 70-22	Coarse Matrix High Binder (CMHB) type F	7.3
Atlanta	Sandstone	PG 76-22	Superpave 12.5mm	5.0
	Quartzite			

The MnROAD 01 Mixture – Superpave 12.5mm (PG 58-34 + Gravel)

The MnROAD 01 mixture was designed with a PG 58-34 binder supplied by Koch Materials. This mix design was used in cell 34 of the MnROAD Research Project test pavement sections. It was primarily designed to field verify the Superpave criteria for low temperature cracking. The PMA contains styrene-butadiene-styrene (SBS) co block polymer interlinked with sulfur. The aggregates were sourced from Danner Incorporated in Saint Paul, Minnesota. It contains three different types of the Danner Rock: Danner ¾ class D, Danner ½ Class D, Danner Crushed Fines, and OttoPed Sand. These components are described in Table 3.2. The aggregate gradation is also shown in Figure 3.1.

Table 3.2 MnROAD 01 and 02 Aggregate Mix Design

Source of Material	Proportions (%)
Danner 1/2" Class D	12
Danner 3/4" Class D	20
Danner Crushed Fines	23
OttoPed Sand	45
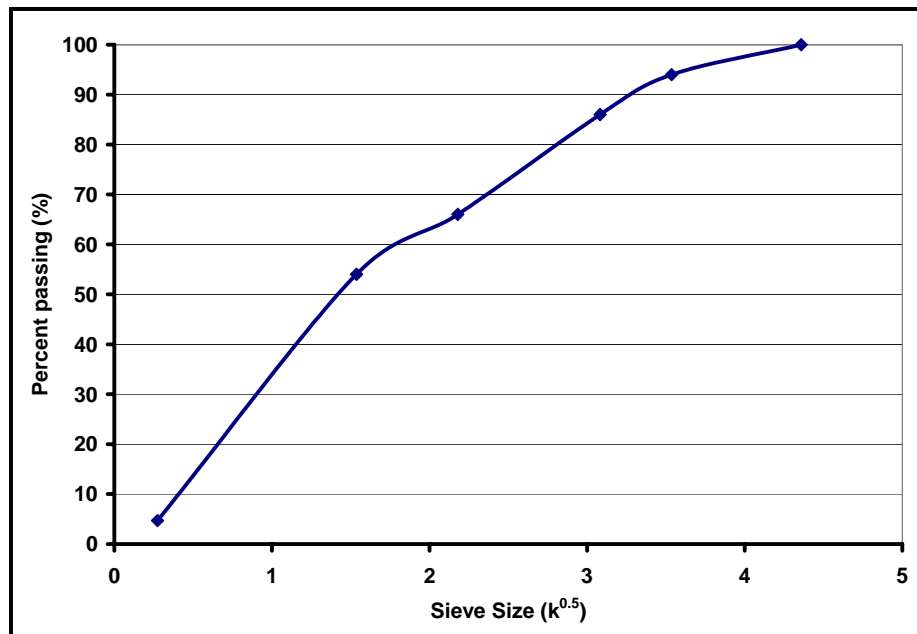
Figure 3.1 Gravel Aggregate Gradation for MnROAD 01 and 02 Mixtures

The MnROAD 02 Mixture – Superpave 12.5mm (PG 58-40 + Gravel)

The MnROAD 02 mixture was designed with a PG 58-40 binder supplied by Koch materials. This mix design was used in cell 35 of the MnROAD Research Project test pavement. The only difference between the MnROAD 01 and the MnROAD 02 is the asphalt binder grade. Whereas in the MnROAD 01 mixture PG 58-34 was used, the

MnROAD 02 mixture used PG 58-40. Thus the aggregate source and gradation are the same as shown in Table 3.1 and Figure 3.1, respectively.

The Waco Mixture – Superpave 19mm (PG 70-22 + Igneous)

The Waco mixture consisted of igneous aggregates and PG 70-22 asphalt supplied by Alon asphalts. This mix design was used for Interstate Highway (IH) 35 in McLennan County in Waco, Texas. The mix design was used with 5.3% asphalt content by weight of the mix, and the HMAC was fabricated to $7 \pm 0.5\%$ air void content. The Superpave 19mm aggregate gradation used for this mix is shown in Figure 3.2. Table 3.3 gives the proportions of aggregate materials used for the gradation shown in Figure 3.2.

Table 3.3 Waco Mixture Aggregate Mix Design

Source of Material	Proportions (%)
Hanson Okl. ¾" Rock	20
Young/Maddox C Rock	18
Young/Maddox F Rock	20
Young/Maddox Screenings	28
Hanson Okl. Screenings	14
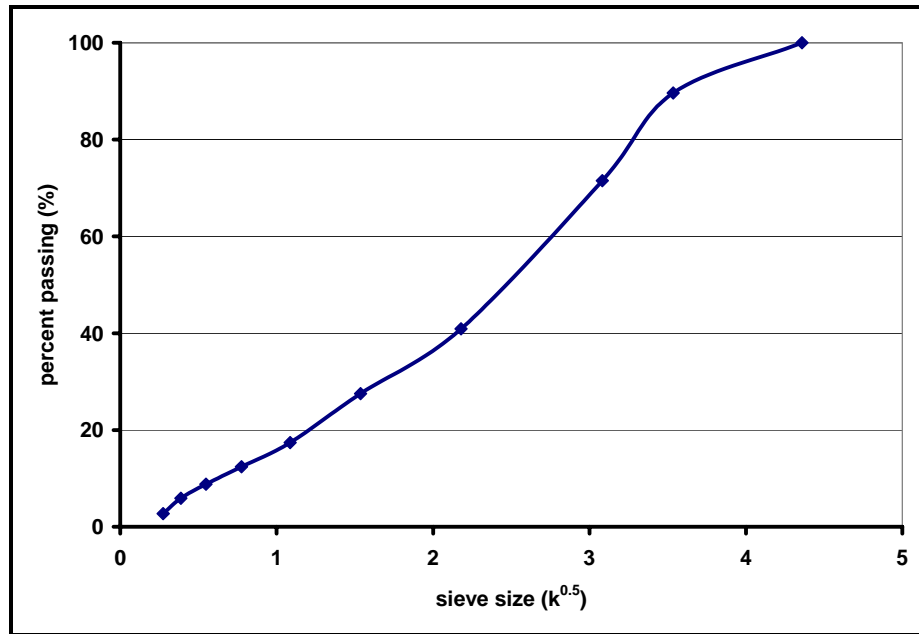
Figure 3.2 Aggregate Gradation for Waco Mixture

The Odessa Mixture – CMHB_F (PG 70-22 + Rhyolite)

The Coarse Matrix High Binder (CMHB) type F mixture is one of the less common mix types used by the Texas Department of Transportation (TxDOT). This mix type was used in the Odessa Mixture. It consists of PG 70-22 supplied by Alon and Hoban Rock aggregates supplied by Jones Mill. The asphalt contains SBS polymer modifier, and the aggregates consist of rhyolite and limestone screenings. This mix was used on the Farm to Market 1936 road section (FM 1936). The CMHB_F aggregate gradation used is shown in Figure 3.3. Table 3.4 gives the proportions of aggregate types that made up the gradation.

Table 3.4 Odessa Mixture Aggregate Mix Design

Source of Material	Proportions (%)
Hoban Grade 4	35
Hoban Grade 6	42
Jones Screenings	23
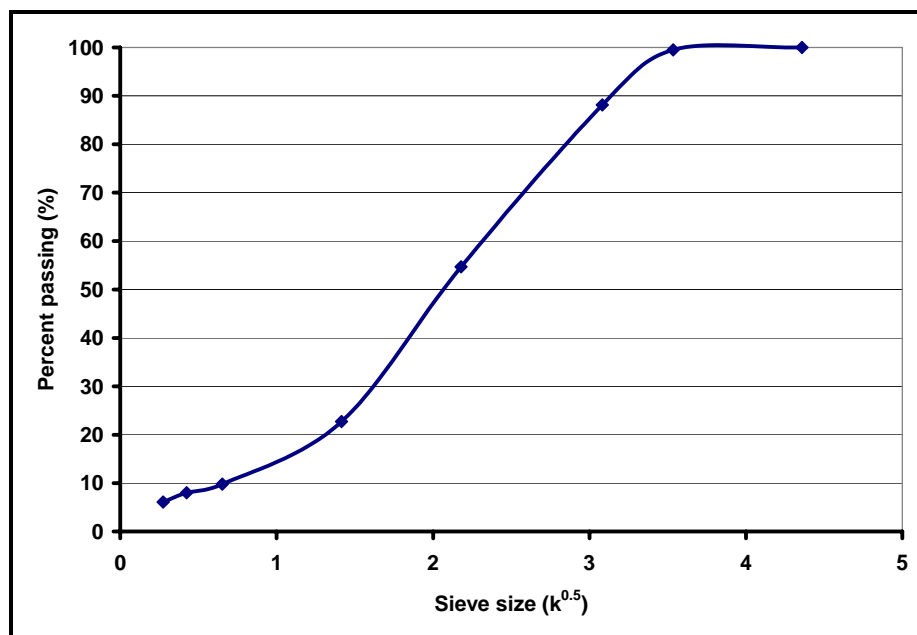
Figure 3.3 Aggregate Gradation for Odessa Mixture

The Atlanta Sandstone Mixture – Superpave 12.5mm (PG 76-22 + Sandstone)

The Atlanta Sandstone mixture was used on IH 20 in Harrison County of the Atlanta district in Texas. Sandstone aggregates obtained from the Meridian Sawyer Quarry were combined with PG 76 – 22 asphalt containing 3 -5% SBS by weight of base asphalt supplied by Wright Asphalt. The asphalt content in the mix design was 5.0% by weight of the total mix. The aggregate gradation of the sandstone aggregates is shown in

Figure 3.4. In this sandstone mix design, 1% hydrated Texas lime was added as antistrip

agent and 8% Granite Donnafill was also added. Table 3.5 shows the different aggregate

components and their corresponding proportions.

Table 3.5 Atlanta Sandstone Mixture Aggregate Mix Design

Source of Material	Proportions (%)
Meridian Type C	22
Meridian Type D	57
Meridian Screenings	12
Ark. Granite Donnafill	8
Hydrated Texas Lime	1
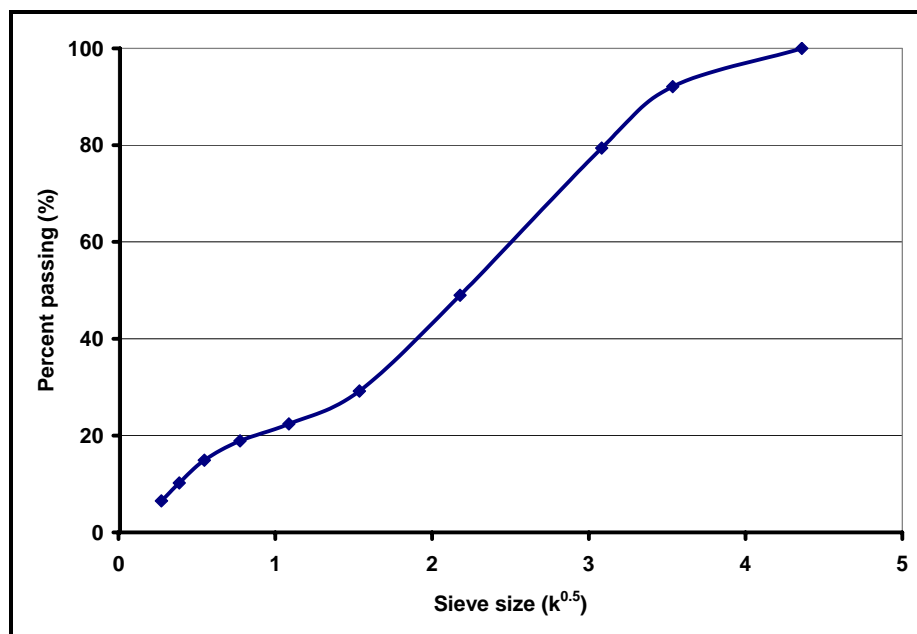
Figure 3.4 Aggregate Gradation for Atlanta Sandstone Mixture

The Atlanta Quartzite Mixture – Superpave 12.5mm (PG 76-22 + Quartzite)

The Atlanta Quartzite mix design was also used on IH 20 in Harrison County in the Atlanta district. These aggregates were sourced from Martin Marietta Jones Mill in Arkansas. The same PG 76-22 as used in the Atlanta Sandstone mixture was used. In the Atlanta Quartzite mix design, however, 10% Granite Donnafill fines was used and 1% hydrated lime was also used as an anti stripping agent. The components in the aggregate structure are shown in Table 3.6, and the aggregate gradation curve is presented in Figure 3.5. The asphalt content by weight of total mix was also 5.0%.

Table 3.6 Atlanta Quartzite Mixture Aggregate Mix Design

Source of Material	Proportions (%)
Martin Marietta Type C	18
Martin Marietta Type D	46
Martin Marietta Screenings	25
Ark. Granite Donnafill	10
Hydrated Texas Lime	1
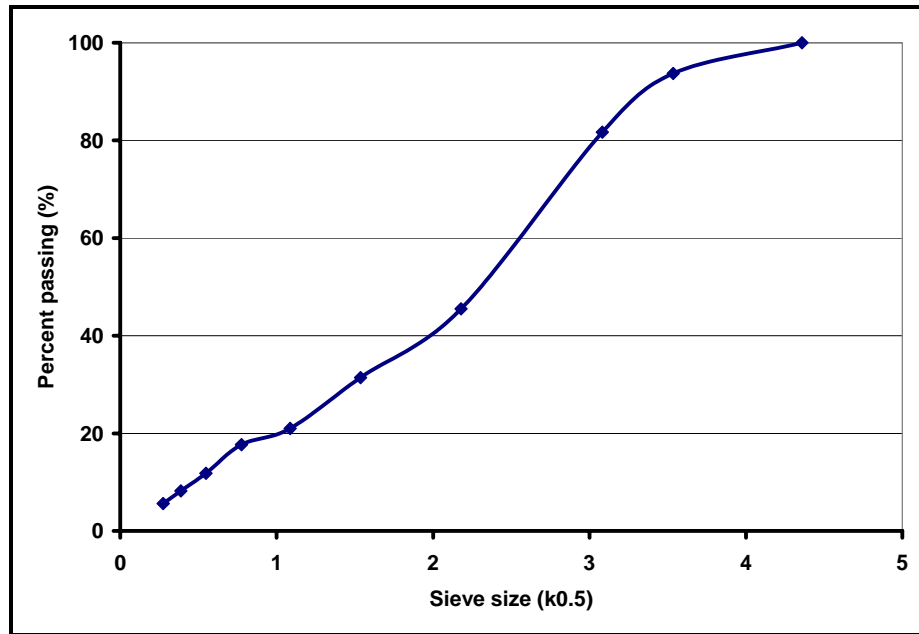
Figure 3.5 Aggregate Gradation for Atlanta Quartzite Mixture

MATERIAL PROPERTIES FOR BINDERS

Asphalt binder characterization was completed to verify the performance grade (PG) of the asphalts. The AASHTO PP1, PP6, T313 and T315 procedures were followed (AASHTO 1998; 1996). The results obtained for the asphalts verified the PG asphalt grades of PG 70-22 and PG 76-22.

MATERIAL PROPERTIES FOR THE AGGREGATES

Aggregate quality tests were completed to ensure that the aggregates supplied met the requirements of TxDOT. These tests were conducted by the aggregate supplier, and Table 3.7 gives a summary of the tests and the specifications required by TxDOT.

Table 3.7 Aggregate Quality Requirements (Texas Specification Guidelines 2004)

PROPERTY	TEST METHOD	SPECIFICATION
STOCKPILE		
Decantation	Tex-217-F Part II	1.5, max
Deleterious material	Tex-217-F Part I	1.5, max
Magnesium Sulfate Soundness	Tex-411-A	30, max
Los Angeles Abrasion	Tex-410-A	40, max
Coarse Aggregate Angularity	Tex-460-A Part I	85, min
Flat and Elongated Particles @ 5:1 % max	Tex-280-F	10, max
FINE AGGREGATE		
Linear Shrinkage	Tex-107-E	3, max
COMBINED AGGREGATE		
Sand Equivalent	Tex-203-F	45, min

Aggregate quality tests were not conducted for the aggregates used in the MnROAD 01 and MnROAD 02 mixtures because they were supplied as loose HMAC.

HMAC SPECIMEN FABRICATION

The various steps taken to complete the HMAC specimen fabrication is outlined below:

Aggregate Sieving and Batching

The aggregates were supplied from stockpiles at the quarry. To separate out individual sizes, they were sieved and then batched according to their gradations as

shown in Figures 3.2 through 3.5. The MnROAD 01 and 02 mixtures were not a part of this process since they were supplied as loose HMA.

Aggregate-Asphalt Mixing and Short Term Oven Aging (STOA)

Batch sizes of aggregates were pre-heated at their respective mixing temperatures shown in Table 3.8 prior to mixing with asphalt. This preheating was done for 4hrs to remove all forms of moisture from the aggregates and to bring the aggregates to their mixing temperature. The respective asphalt binders were also liquefied for about 30 minutes at the mixing temperature. The aggregates and the asphalt were mixed in a rotating bucket until such a time that the asphalt had sufficiently coated the surface of the aggregates. The asphalt-aggregate mixture was then short term oven aged (STOA) for 2hrs at 135°C for the determination of the maximum specific gravity and 4hrs at the same temperature for compaction. The STOA was done according to the AASHTO PP2 protocol (AASHTO 1994).

Theoretical Maximum Specific Gravity Determination

A representative sample of the mixture which had been STOA for 2 hrs was used to determine the maximum specific gravity. This was to enable the computation of the percent air voids (AV) and percent voids in mineral aggregates (VMA) of the compacted HMAC. The Tex-207-F protocol was used to determine the maximum specific gravity. The maximum specific gravity of the MnROAD 01 and MnROAD 02 mixtures were also determined after STOA.

HMAC Compaction

The STOA asphalt-aggregate mixture was compacted using the SGC at the compaction temperature as shown in Table 3.8. The compaction was done according to

the Tex-241-F protocol. The mixtures were compacted to a cylindrical specimen size of 177.8mm height × 152.4mm diameter to a target air voids (AV) content of 10 ± 0.5 percent. After this initial dimension, the HMAC is further sawed and cut to the final dimensions shown in Figure 3.6. In the case of MnROAD 01 and 02, the loose HMA supplied by the MnDOT was compacted using the same protocol to the same dimensions as for the Texas HMAC.
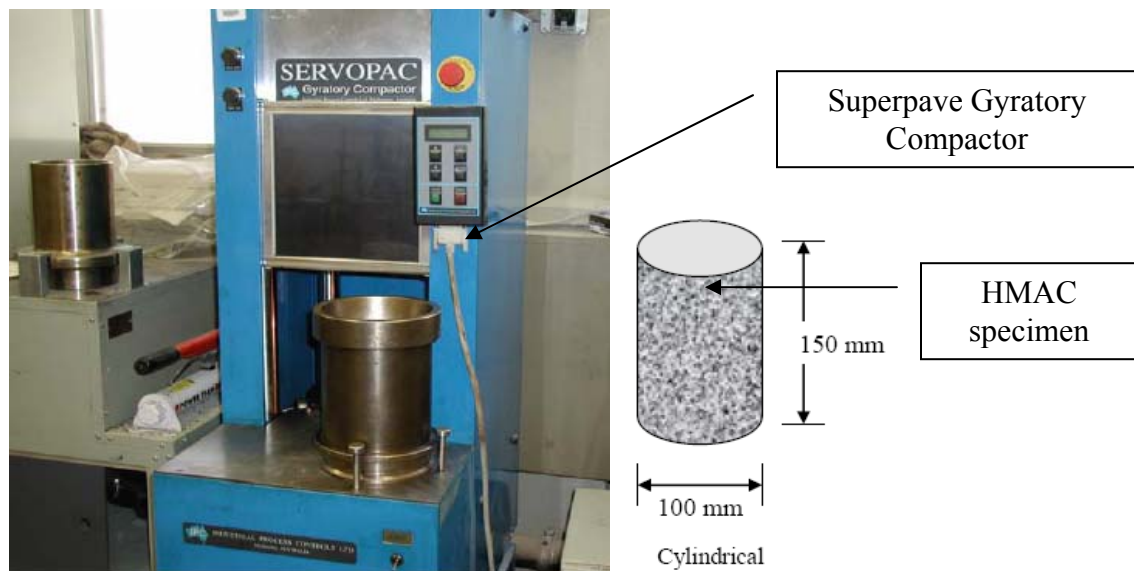
Figure 3.6 Superpave Gyratory Compactor

Table 3.8 HMAC Fabrication Process Temperatures

Process	Temperatures (°C)			
	MnROAD 01	**MnROAD 02**	**Waco & Odessa**	**Atlanta Sandstone & Quartzite**
Aggregate pre-heating	N/A	N/A	149	163
Binder Liquefying	N/A	N/A	149	163
Binder-Aggregate Mixing	N/A	N/A	149	163
STOA	135	135	135	135
Compaction	118	122	135	149

Specimen Sawing, Coring and Air Voids Determination

The bulk specific gravity of the compacted HMAC specimens were determined according to AASHTO PP19 (AASHTO 1993). Volumetric analysis was done to determine the AV contents according to AASHTO T166 (AASHTO 2000). The specimens which passed the target AV of 10 ± 0.5 were then sawed and cored to the dimensions shown in Figure 3.6. AASHTO T166 and PP19 were then used to determine the final AV contents after sawing and coring.

Specimen Storage and Aging

As part of the research, the effect of oxidative aging on the fatigue resistance of HMAC was studied. To determine this effect, the HMAC specimens were aged at 60°C in an environmental room (ER) for three aging periods: 0, 3 and 6 months. According to Glover et al. (2005), these conditions shown in Table 3.9 simulate from 0 – 12 years field aging in Texas pavements.

Table 3.9 Aging of HMAC Specimens (Glover et al. 2005)

Aging Period (months)	Aging Condition	Field Simulation
0	4hrs STOA @ 135C + compaction + 0 months aging in the 60C, 1atm ER	Freshly compacted HMAC pavement layer
3	4hrs STOA @ 135C + compaction + 3 months aging in the 60C, 1atm ER	3 – 6 years Texas HMAC exposure
6	4hrs STOA @ 135C + compaction + 6 months aging in the 60C, 1atm ER	6 – 12 years Texas HMAC exposure

The fabricated HMAC specimens which did not require any aging were stored on flat surfaces in a controlled room temperature environment. The HMAC specimen storage and aging is shown in Figures 3.7 and 3.8.

Figure 3.7 HMAC Specimen Storage

Figure 3.8 HMAC ER Aging

HYPOTHETICAL PAVEMENT STRUCTURE AND TRAFFIC PARAMETERS

To determine the fatigue resistance of the HMAC mixtures used in this research, a hypothetical pavement structure was selected and used for comparison. This pavement structure is shown in Figure 3.9. According to Freeman (2004) for this structure, common traffic loading parameters include an 80kN (18kip) axle load, 690kPa (100psi) tire pressure, 97km/hr (60mph) vehicle speed, and 10-25% truck traffic. These components were used at a traffic design level of 5×10^6 ESAL for a 20 year design life of the pavement structure. These traffic input parameters were used in ELSYM5, a layer elastic model, to compute the critical design strains for the pavement structure. The computed strains were then adjusted using a Finite Element Method to account for the visco-elasticity and plastic behavior of the HMAC layer. Table 3.10 shows the traffic loading parameters chosen and the computed critical design strains.

Table 3.10 Traffic Loading Parameters and Critical Design Strains

Description	Traffic Parameters		Critical Design Strains	
	ESALs	% Trucks	ε_t	γ
Pavement Structure	5×10^6	25	1.57×10^{-4}	1.56×10^{-2}
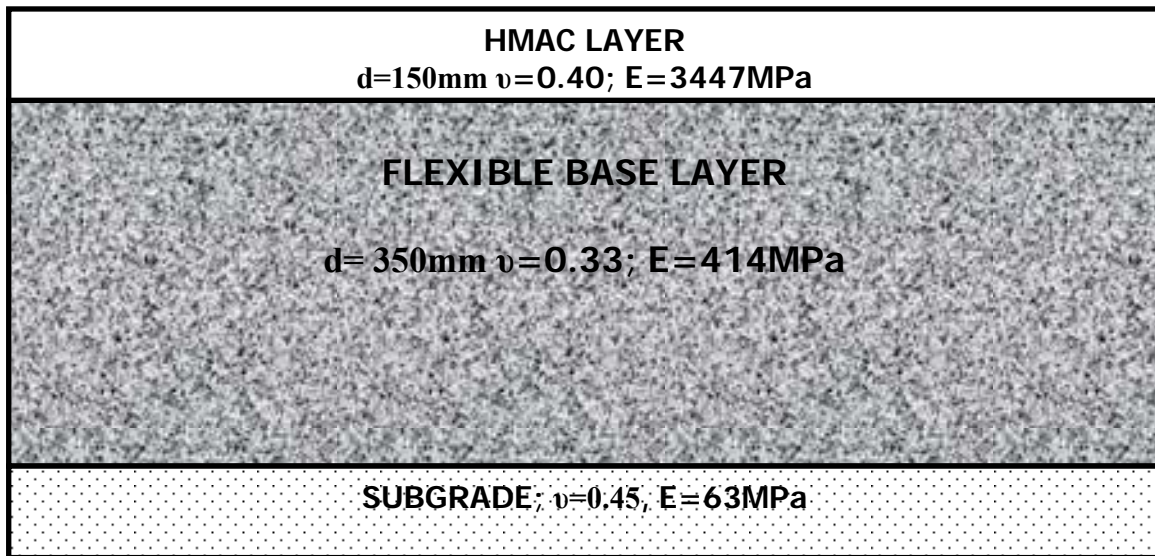
Figure 3.9 Hypothetical Pavement Structure

ANALYTICAL MEASUREMENTS

The HMAC specimens were tested according to the CMSE test protocol. This involved the measurement of surface energy components of the aggregates and binder separately, tensile strength measurements, relaxation modulus measurements in tension and compression, and the uniaxial repeated direct tension measurements. These testing protocols are described in this section. A more detailed description can be found elsewhere (Walubita 2006).

Another objective of this research was to establish the influence of aggregate geometric properties on the fatigue resistance of HMAC. In this regard, the Aggregate Imaging Measurement System (AIMS) was used to determine the shape, angularity, and texture properties of the aggregates used. The AIMS procedure is also discussed briefly in this section with an in-depth description found elsewhere (Alrousan 2004).

Aggregate and Binder Surface Energy

The ability of a liquid to wet the surface of a solid is an important feature in determining the compatibility of an asphalt binder aggregate system. If the intermolecular forces within the asphalt binder are stronger than that between the aggregate and the asphalt binder, then wetting of the surface of the aggregate by the asphalt binder will occur. One way of determining the wetting ability of the asphalt is to determine its contact angle with a surface.

The Wilhelmy Plate (WP) Method shown in Figure 3.10 method was used to determine the contact angles that the asphalt binder made with a micro cover glass slide. This WP method works on the principle that the contact angle the asphalt coated micro glass cover makes with a probe liquid after correcting for buoyancy can be used as a measure of its surface energy components. The asphalt is first liquefied and a thin film coated onto the micro glass cover and used for this test. The coated glass slides were de-aired in a dessicator overnight prior to the test. Through immersion and withdrawal of the coated micro glass cover, the advancing and receding contact angles with the probe liquid were measured and facilitate calculation of the healing and fracture surface energies. The probe liquids used in these measurements were water, glycerol and formamide. Two replicate test specimens per probe liquid per asphalt were measured. The protocol

followed in the determination of the advancing and receding contact angles of the asphalt binder to the glass slides as well as the empirical equations used to compute the surface energy components of the asphalts are discussed extensively elsewhere (Cheng 2002; Walubita 2006; Bhasin 2006).

The asphalts were subjected to a Stirred Air Flow Test (SAFT) for aging and subsequently aged in the ER for 0, 3, and 6 months to simulate aging in the pavements. The aged specimens were also tested with the WP to determine their surface energies.

Wilhelmy Plate (SE) Apparatus in use

Figure 3.10 Wilhelmy Plate Test Set-up

To determine the aggregate surface energy, the Micro calorimeter (MC) device shown in Figure 3.11 was used. This method works on the principle that the measure of enthalpy of immersion of aggregates in different probe liquids is an indication of the surface free energies of the aggregates. In using this device it was necessary that adequate specific surface area of the aggregates were available to generate heat of immersion which is measured by the MC. Thus crushed aggregate particles passing sieve size # 100 and retained on the #200 sieve were used for this test. The aggregate particles were washed with distilled water on the sieve size # 200 and oven dried to remove all forms of debris, dust and moisture. The three probe liquids used in this test were heptane, benzene,

and chloroform. At least two replicate measures were made per probe liquid per aggregate type. A more detailed description of the theory and principles underlying this approach is found elsewhere (Bhasin 2006). On the assumption that aggregate properties do not change with aging, this test was done only for the 0 months aging condition. A detailed step by step of the WP and MC procedure used is given in Appendix A.

Supporting software for MC

Prepared aggregate samples ready for test

Micro Calorimeter Test Apparatus
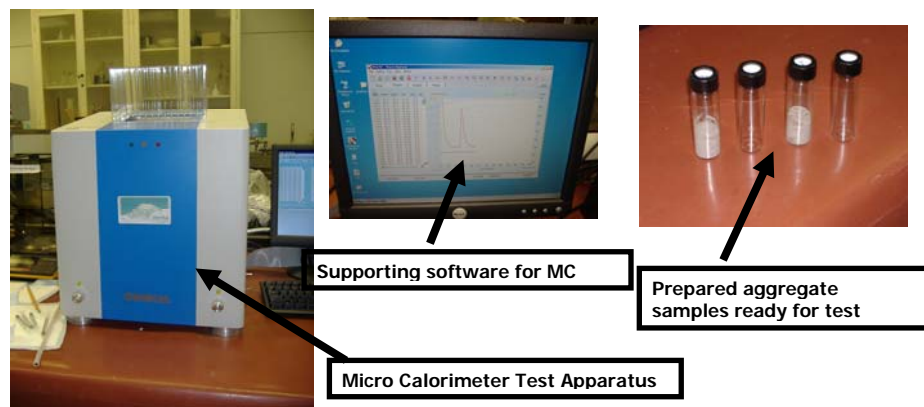
Figure 3.11 Micro Calorimeter Test Set-up

Aggregate Imaging Measurement System (AIMS)

AIMS was developed by Dr. Masad of the Texas Transportation Institute and is a promising methodology to characterize aggregate shape, form and texture. The results from AIMS have been shown to have a direct relationship with the fundamental factors governing pavement performance. The results from AIMS have also shown repeatability and reproducibility (Bathina, 2005).

The test equipment for AIMS is shown in Figure 3.12. The detailed description of the test methodology and equipment is found elsewhere (Alrousan, 2004 and Bathina, 2005).

Figure 3.12 AIMS Set Up

A test sample consisting of 56 particles for coarse aggregates was placed on specified grid points on the measurement tray for scanning. For the fine aggregates, a handful of the aggregates were spread uniformly on the measurement grid for scanning. A built-in camera unit captures images of the aggregates in black, white and gray format; and an attached software system evaluates the images and determines aggregate texture, angularity, sphericity and 2D form. For fine aggregate, 2D form and angularity are the only properties captured, as angularity and texture in fine aggregates has a direct correlation (Masad, 2001). For coarse aggregates, shape, texture, sphericity, 2D form and angularity properties are determined.

The analysis of the scanned results is based on the captured images of the aggregate particles during the scan. A total description of the analysis process is reported elsewhere (Alrousan, 2004 and Bathina, 2005). The indices measured from this

methodology are Angularity Index (radius and gradient methods), Form Index, Sphericity Index and Texture Index.

Each aggregate type was wet sieved and separated into particle sizes. Particles retained on sieve sizes ½", 3/8" and #4 were classified as coarse aggregates and were scanned for their texture, angularity and 2D form. Particle sizes which were retained on sieve sizes #8, #16, #30, #50 and #100 were classified as fine aggregates and scanned for their angularity and 2D form only. All particle sizes were washed thoroughly with distilled water to remove all forms of dust and debris which are possible sources of error in the measurements. Two replicate test samples per particle size per aggregate type were scanned and measured using AIMS.

HMAC Tensile Strength (TS) Measurements

A tensile strength test to determine tensile strength of the HMAC was conducted on HMAC specimens at 20°C. The test was conducted in a temperature controlled chamber while using a thermocouple inserted into a dummy sample to monitor the fluctuation of temperature in the chamber. At a loading rate of 0.05in/min, tensile load was applied axially to the HMAC specimen until failure. The tensile strain accompanying the increasing tensile load was measured electronically every 0.1s until failure using Linear Variable Displacement Transducers (LVDTs). The maximum tensile stress (σ_t) the HMAC material could withstand before failure and the corresponding failure strain (ε_f) for each HMAC specimen was determined. Prior to testing the HMAC specimens were temperature conditioned for a minimum of 4 hours at the testing temperature of 20°C. Two replicate measurements per HMAC specimen per aging condition were taken. A pictorial representation of the test protocol is shown as part of Figure 3.13.

HMAC Relaxation Modulus (RM) Measurements

A Relaxation Modulus (RM) test in tension and compression was done on the HMAC specimens at 10°C, 20°C, and 30°C to determine the relaxation properties of the HMAC at the different temperatures. The RM is a strain controlled test and thus axial loading in tension and compression was applied to the specimen to determine the relaxation parameters E_t and m_t for tension and E_c and m_c for compression. The axial loading was applied for 6 seconds to reach a 200microstrain level which is 20% of the failure tensile strain in the HMAC, and a relaxation period of 60s was allowed both for the tension and compression. The RM test was also conducted in a temperature controlled chamber, and a thermocouple inserted into a dummy sample was used to monitor the fluctuation of temperature in the chamber. The strains in the HMAC specimen during the test were collected electronically every 0.5s using LVDTs attached vertically to the sides of the specimen. Prior to testing the HMAC specimens were temperature conditioned for a minimum of 4 hours at the testing temperature of 10°C, 20°C, and 30°C, respectively. The relaxation parameters were then determined by forming a master curve at 20°C and using a Sum of Squared Errors (SSE) approach. Two replicate measurements per HMAC specimen per aging condition per test temperature were taken. A pictorial representation of the test protocol is shown as part of Figure 3.13.

HMAC Uniaxial Repeated Direct Tension (RDT) Measurements

The RDT test procedure was done on the HMAC specimens to measure the rate of accumulation of Dissipated Pseudo Strain Energy (DPSE) in the specimen. A strain controlled uniaxial repeated direct tension load was applied to the HMAC specimens at 20°C at a specific micro strain level. For the Waco, Odessa, Atlanta Sandstone, and

Atlanta Quartzite the strain level was 350microstrain whereas it was 200microstrain for the MnROAD 01 and 02 mixtures. These strain levels represent 35% and 20% of their respective failure tensile strain in the TS test. These strain levels were determined to be enough to induce micro cracking in the specimen. An input haversine load form representative of the load pulse developed under traffic loads was applied. The test was conducted in a temperature controlled chamber, and a thermocouple inserted into a dummy sample was used to monitor the temperature fluctuation in the chamber. At a loading frequency of 1Hz, the test was terminated at 1000 loading cycles where a full cycle consisted of 0.1s loading time and 0.9s rest period. LVDTs were used to capture the strains developed in the HMAC specimen during the test while the loading was applied by means of an MTS loading cell. Temperature conditioning for 4 hrs was done prior to testing, and two replicate measurements per aging condition were completed. The RDT test was done on the same specimens which were tested for RM.
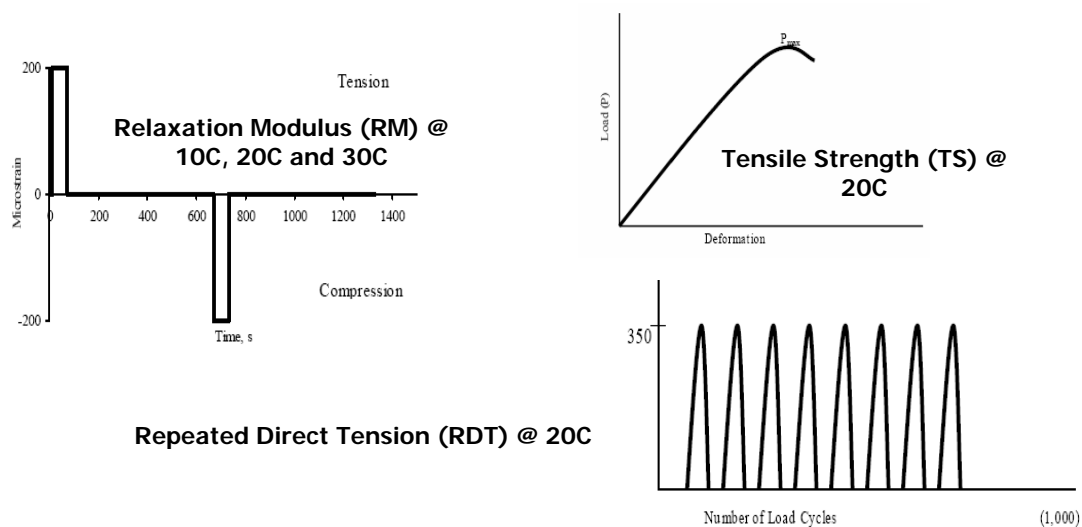
Figure 3.13 CMSE Mixture Test Protocols

ANALYSIS PROCEDURE

Introduction

The CMSE approach of fatigue life determination relies on the principle that loading the HMAC layer repeatedly induces micro crack initiation and then propagation through the HMAC layer. However, the bond strength of the asphalt aggregate matrix allows healing of the micro cracks as they are formed. It is fundamentally based on the Schapery modified Work Potential Theory and Paris' Law of Fracture. This approach also accounts for the fact that HMAC is a heterogeneous material and as such exhibits anisotropy. As a result the fatigue life of HMAC according to this approach is a function of anisotropy, healing, number of load cycles to crack initiation and number of load cycles to crack propagation through the HMAC layer. The CMSE uses fundamental material properties to determine the fatigue resistance of a mixture. The failure criterion in this approach is the growth and propagation of a 7.5mm crack through the HMAC layer according to Lytton et al. (1993).

The CMSE approach is explained in detail elsewhere (Walubita 2006) but the primary equations used to determine fatigue life are described in this section.

Material Property Outputs from Laboratory Tests

A summary of the material properties used in the CMSE approach and determined from the laboratory tests is as follows:

- Tensile Strength (TS) test

    o σ_t (Tensile Strength), ε_f (failure strain)

- Relaxation Modulus (RM) test

- o E_t (Relaxation Modulus in Tension), m_t (relaxation rate in tension), E_c

  (Relaxation Modulus in compression), m_c (relaxation rate in compression),

- Repeated Direct Tension (RDT) test

  - o b-value (slope of the DPSE versus Log of load cycles plot)

- Surface Energy tests

  - o ΔG_h (Bond Strength of the asphalt-aggregate due to healing), ΔG_f (Surface

    Energy of the asphalt-aggregate mixture due to fracture)

Determination of Fatigue Life N_f from Laboratory Test Outputs

Based on the outputs from the laboratory tests, the fatigue lives of the HMAC

mixtures were determined using the following equations 3.1 through 3.8:

$$N_f = SF_i \left(N_i + N_p \right) > Q \times TrafficDesign(ESALs) \dots\dots(3.1)$$

N_f − Fatigue Life

$$SF_i = SF_a \times SF_h \dots\dots(3.2)$$

$$SF_a = \left(\frac{E_z}{E_x} \right)^{1.75} \dots\dots(3.3)$$

SF_a − Shift factor due to anisotropy

$$SF_h = 1 + g_5 \left(\frac{\Delta_{tr}}{a_{TSF}} \right)^{g_6} \dots\dots(3.4)$$

SF_h − Shift factor due to healing

g_5, g_6 − fatigue calibration constants

a_{TSF} − temperature shift factor for field conditions

Δ_{tr} − rest periods between major traffic loads

$$n = \frac{1}{m} \quad\text{...(3.7)}$$

n & m as previously defined

$$N_p = \left[\frac{d^{1-n/2}}{A(2r)^n (SG)^n (1-nq)} \right]\left[1-\left(\frac{C_{max}}{d}\right)^{1-nq} \right]\left(\frac{1}{\gamma}\right)^n \quad\text{...(3.8)}$$

N_p – number of load cycles to crack propagation

d - HMAC layer thickness

γ – design shear strain

r, q - regression constants

S, G - Shear coefficient and modulus respectively

$$N_i = \left(\frac{C_{max}^{1+2n}}{A}\right)\left(\frac{4\pi A_c}{b}\right)^n C_D^{\ n} \quad\text{...(3.5)}$$

N_i – number of load cycles to crack initiation

C_{max} – maximum micocrack length 7.5mm

A & n - Paris' Law Fracture coefficients

b - rate of accumulation of DPSE

C_D – maximum crack density

A_C – cross - sectional area of the HMAC

$$A = \left[\left(\frac{k}{\sigma_t^{\ 2} I_i}\right)\left(\frac{D_1^{1-m} E_t}{\Delta G_f}\right)^{\left(1/m\right)\left(\frac{1}{1+n_{BD}}\right)} \int_0^{\Delta t} w^n(t)dt \right] \quad\text{..(3.6)}$$

k, I, n_{BD} – material coeffiients

D - creep compliance of the HMAC

E_t, m – as from RM test

σ_t – as from TS test

ΔG_f – as from SE test

SUMMARY

This chapter outlines the methodology adopted in this research. Highlights of the chapter concentrated on the experimental design, the material properties, HMAC specimen fabrication, analytical CMSE measurements and a summary of the analysis procedure adopted to compute the fatigue lives of the HMAC.

CHAPTER IV

LABORATORY TEST RESULTS AND ANALYSIS

The laboratory test results and analysis are presented in this chapter. This includes the tests done on the aggregates and asphalt binders and the HMAC mixture tests. Where there was the need to evaluate the effects of aging on the properties of these components, the results for the three oxidative aging conditions used in this study are presented. The chapter is presented in the following sequence:

- AIMS Test Results

- Surface Energy Results

- HMAC CMSE Test Results

    - Tensile Strength Results

    - Relaxation Modulus Results

    - Uniaxial Repeated Direct Tension Results

AIMS TEST RESULTS

AIMS was used to measure the geometric properties of the aggregates including surface texture, gradient angularity, 2D form, and sphericity. In determining these properties, different particle sizes used in the aggregate gradation were scanned. A spreadsheet incorporated in the AIMS analysis system produced a cumulative distribution of the property index versus the percentage of particles for all the different particle sizes. A combined report was then generated giving the total particles scanned, the average

property index of all the particles as well as other statistical parameters such as the standard deviation, the mode and the median. The values in Table 4.1 represent the average values from the combined report. Two replicate scans were taken per aggregate type and size. Appendix B presents the complete AIMS results for all aggregates scanned.

Table 4.1 Aggregate Geometric Properties for MnROAD Aggregate Types

Aggregate Property	MnROAD Gravel			
	Danner 1/2" Class D	Danner 3/4" Class D	Danner Crushed Fines	OttoPed Sand
Texture	194.90	187.55	172.80	121.55
Gradient Angularity	2881.70	3003.25	3228.40	2550.28
Sphericity	0.680	0.690	0.600	0.701
2D Form	7.50	7.45	8.10	7.10

For the MnROAD Gravel, the particles were scanned as used in the aggregate gradation. Thus they were scanned as particle size per aggregate type. Using the same proportions as in the mix design, the mean aggregate property indices were determined as weighted averages and the results are shown in Table 4.2.

Table 4.2 Mean Aggregate Geometric Property Indices

Aggregate Property	Aggregates				
	MnROAD	Waco	Odessa	Atlanta Sandstone	Atlanta Quartzite
Texture	176.08	134.51	192.54	139.37	171.37
Gradient Angularity	3224.02	2841.19	2600.21	3410.19	2968.15
Sphericity	0.745	0.742	0.759	0.746	0.690
2D Form	8.42	7.40	7.05	8.05	8.06

Figures 4.1, 4.2, 4.3, and 4.4 give a summary of the property indices of each aggregate used in the mixtures. They are plotted in an ascending order for each property index. These property indices were measured to aid in the understanding of the role of aggregates in the fatigue performance of HMAC mixtures.
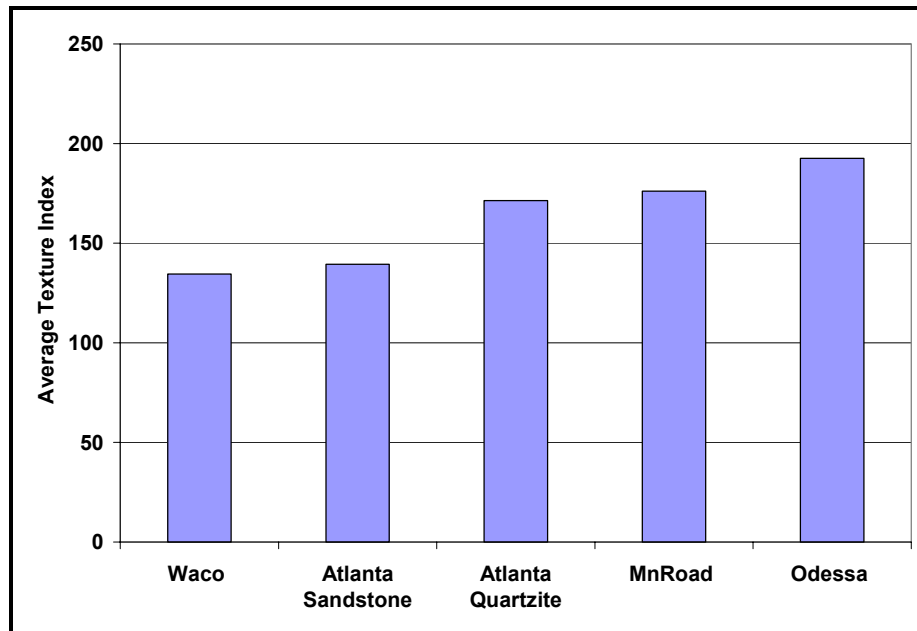
Figure 4.1 Aggregate Surface Texture Index
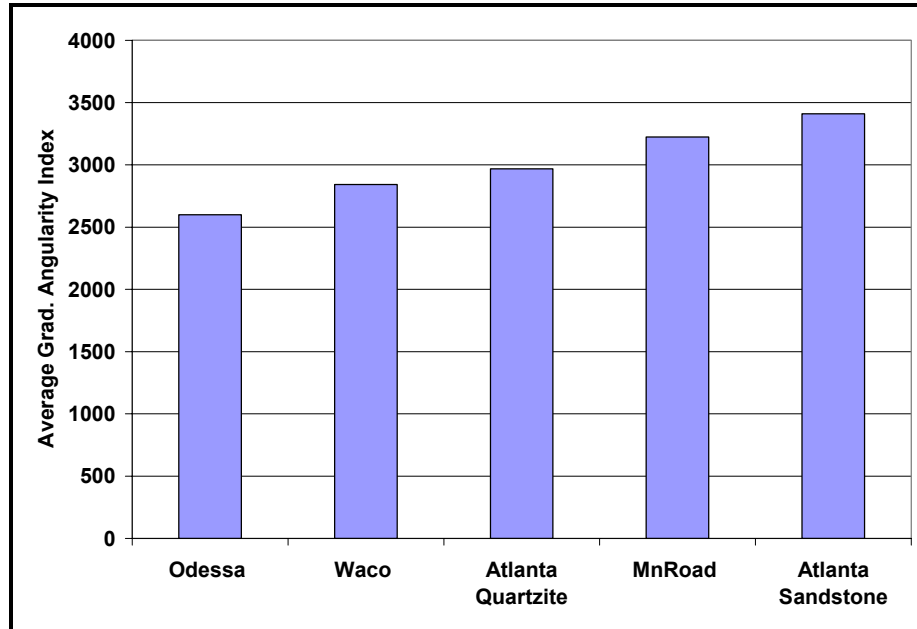
Figure 4.2 Aggregate Gradient Angularity Index
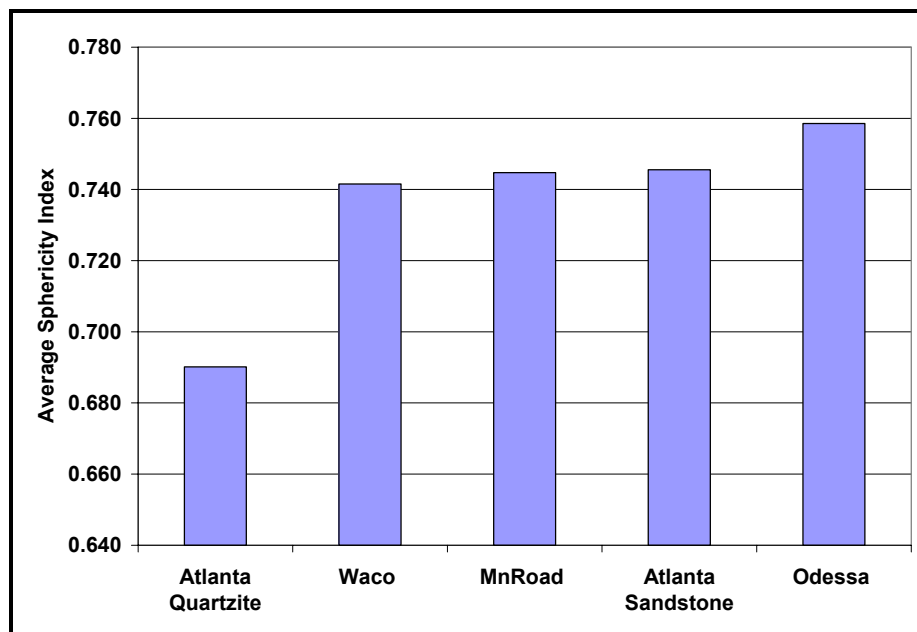
Figure 4.3 Aggregate Sphericity Index
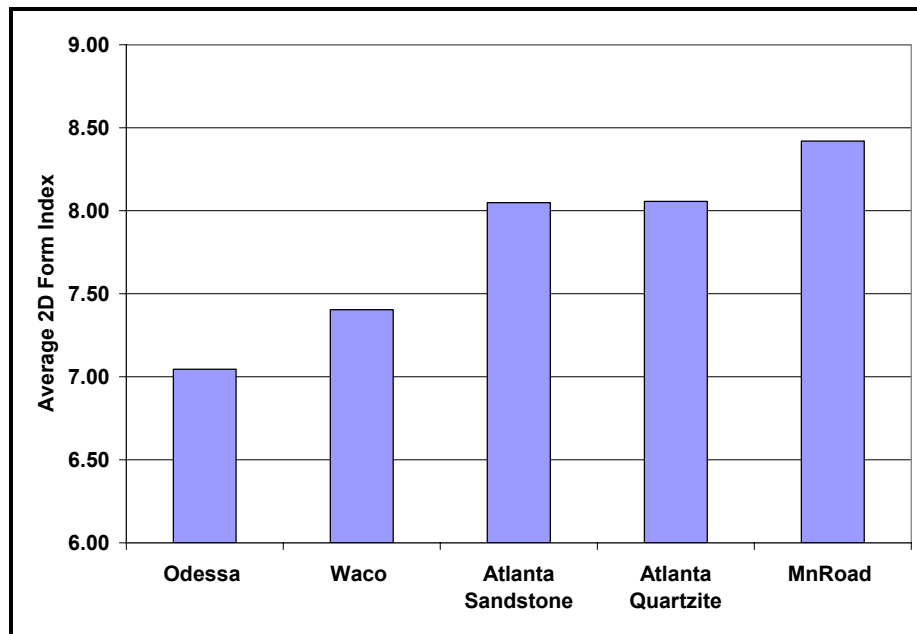
Figure 4.4 Aggregate 2D Form Index

To enable comparison and classification of the aggregate types, a reference scale was developed for all the property indices determined using AIMS. Table 4.3 gives the classification ranges for the various properties measured.

Table 4.3 Aggregate Geometric Property Reference Scale

Aggregate Geometric Property	Range and Description				
Texture Scale	High Roughness	Moderate Roughness	Low Roughness	Smooth	Polished
	> 460	350 - 460	275 - 350	165 - 275	< 165
Gradient Angularity	Angular	Sub-Angular	Sub-Rounded	Rounded	
	> 5400	3975 - 5400	2100 - 3975	< 2100	
Sphericity	H. Sphericity	M. Sphericity	L. Sphericity	Flat/Elongated	
	> 0.8	0.7 - 0.8	0.6 - 0.7	< 0.6	
2D Form	Circular	Semi-Circular	Semi-Elongated	Elongated	
	< 6.5	6.5 - 8	8 - 10.75	> 10.75	

SURFACE ENERGY TEST RESULTS

The surface energy components of the asphalt and aggregates were measured separately. The adhesive aggregate-asphalt bond strength (ΔG) was then computed for each asphalt-aggregate pair. Fracture Bond Strength (ΔG_f) is a measure of the energy needed to create a crack between the asphalt and aggregate, whereas Healing Bond Strength (ΔG_h) is a measure of the energy needed to heal the fracture surface between the asphalt and aggregates. These two aggregate-asphalt bond energies have two components each; the acid-base component (ΔG^{AB}) and the Lifshitz Van-der Waal's component (ΔG^{LW}) as given in Equations 4.1a and b.

$$\Delta G_f = \Delta G_f{}^{LW} + \Delta G_f{}^{AB} \dots\dots\dots\dots\dots\dots\dots\dots\dots\dots\dots\dots\dots\dots (4.1a)$$

$$\Delta G_h = \Delta G_h{}^{LW} + \Delta G_h{}^{AB} \dots\dots\dots\dots\dots\dots\dots\dots\dots\dots\dots\dots\dots\dots (4.1b)$$

ΔG_h^{LW} is related inversely to the short term healing rate, and ΔG_h^{AB} is related to the long term healing rate. The higher the ΔG_f, the greater the resistance of the aggregate-asphalt mixture to fracture. ΔG_f and ΔG_h^{LW} both decrease in magnitude with aging, whereas the magnitude of ΔG_h^{AB} increases with aging.

The trend observed in Figure 4.5 indicates that MnROAD 01 has greater resistance to fracture at 0 and 6 months aging conditions than the MnROAD 02 mixture. The observation for the 3 months aged specimen is not clear as to which mixture is better. In Figure 4.6, MnROAD 01 is expected to heal micro cracks better in all three aging conditions as compared to MnROAD 02. In terms of their long term healing rate characteristics, Figure 4.7 shows that MnROAD 01 has better attributes. In summary, MnROAD 01 is expected to perform better in terms of fatigue resistance compared to MnROAD 02 based on the bond strength results.
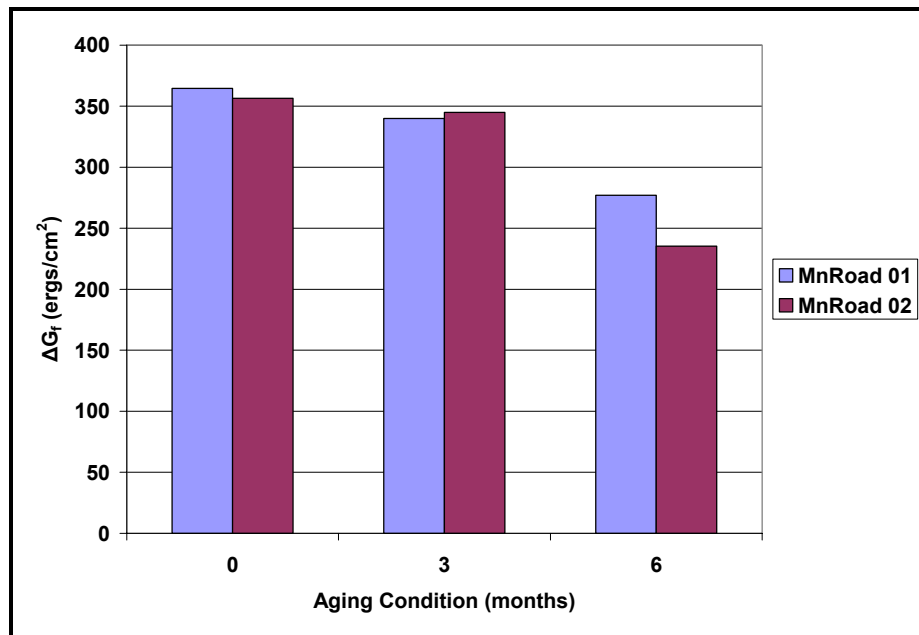
Figure 4.5 MnROAD 01 and 02 ΔG_f with Aging
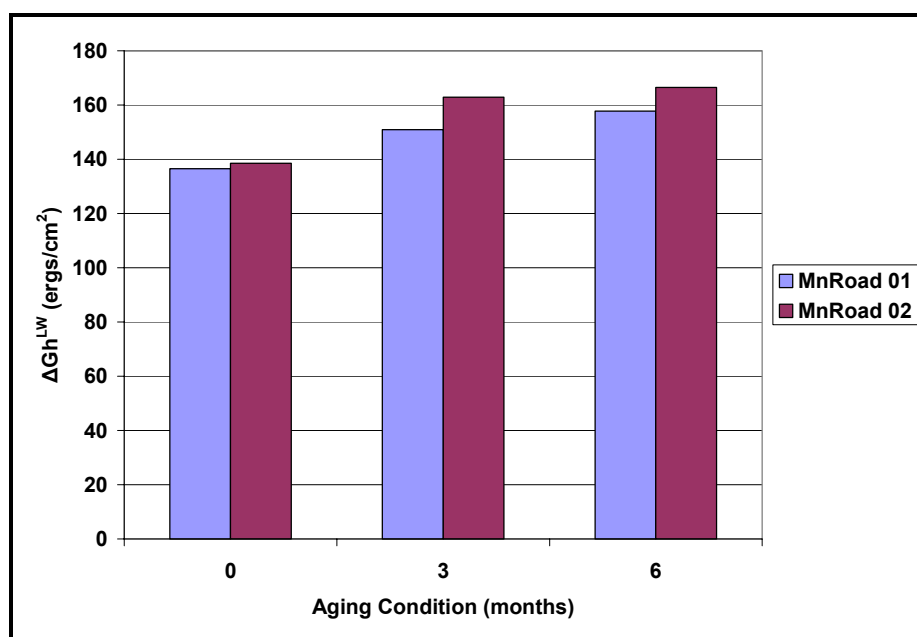
Figure 4.6 MnROAD 01 and 02 ΔG_h^{LW} with Aging
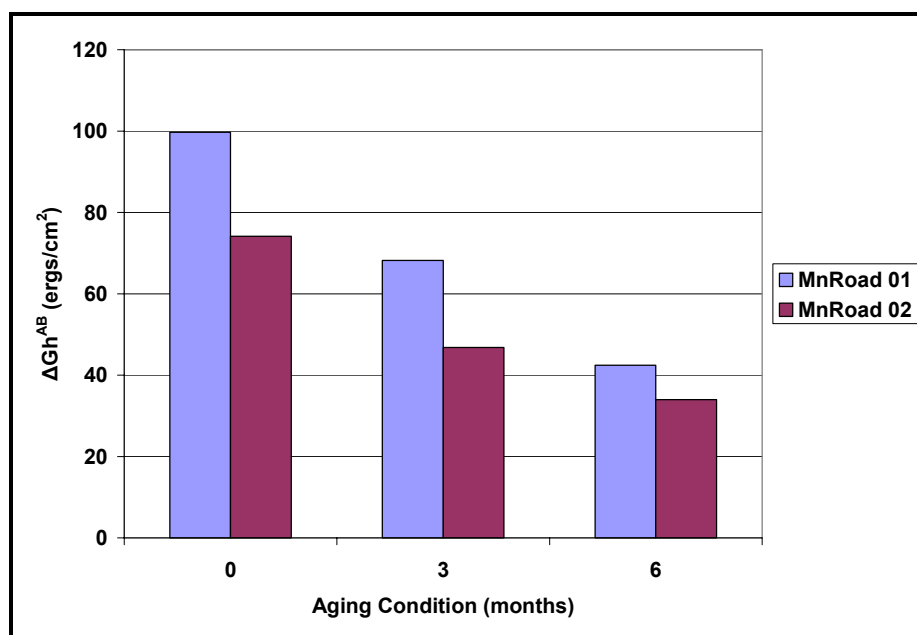
Figure 4.7 MnROAD 01 and 02 ΔG_h^{AB} with Aging

Figures 4.8, 4.9, and 4.10 indicate the Waco mixture as better in terms of the surface energy indicators of fatigue resistance as compared to the Odessa mixture. In all three adhesive surface energy components compared in all three aging conditions, the Waco mixture exhibited superior characteristics over the Odessa mixture.
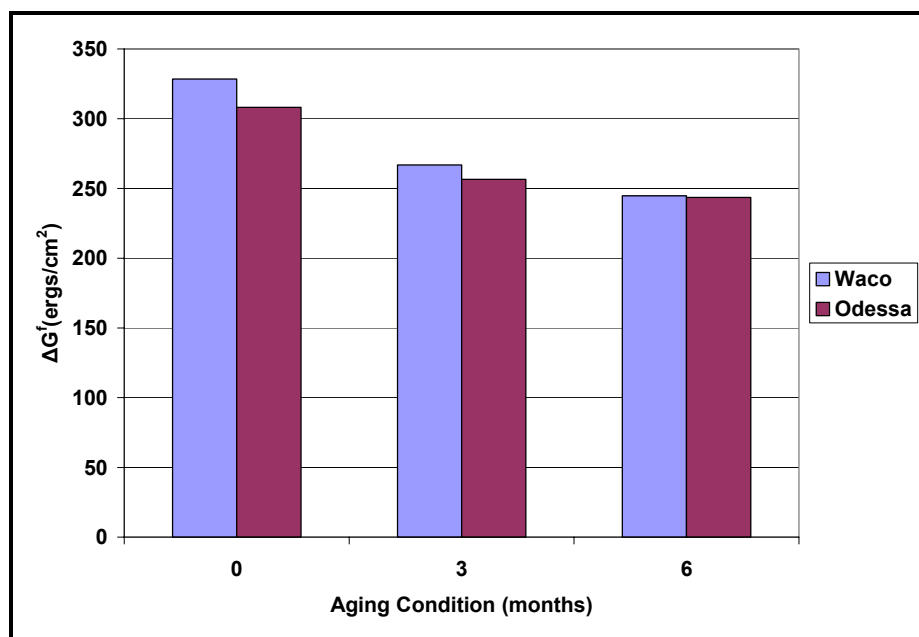
Figure 4.8 Waco and Odessa ΔG_f with Aging
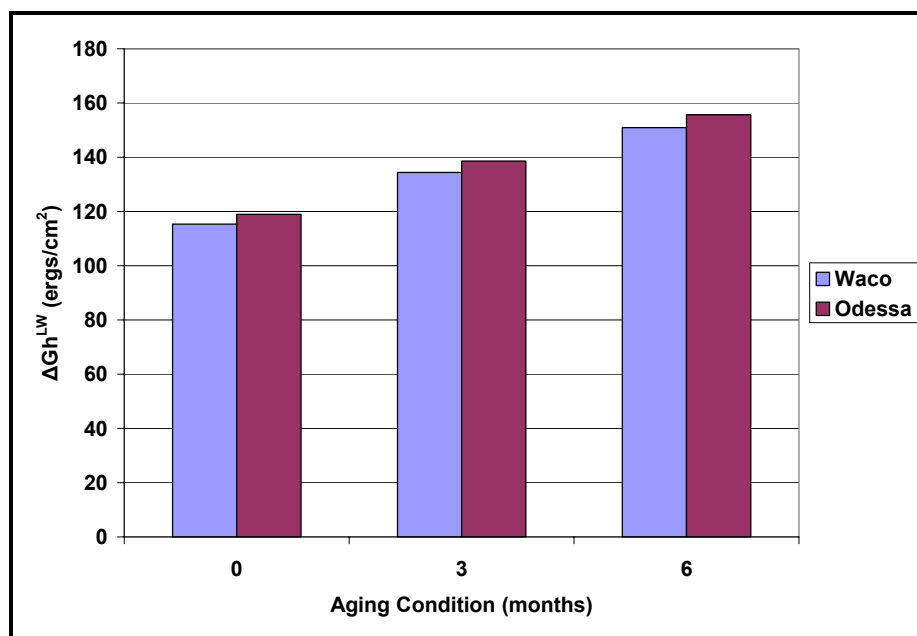
Figure 4.9 Waco and Odessa ΔG_h^{LW} with Aging
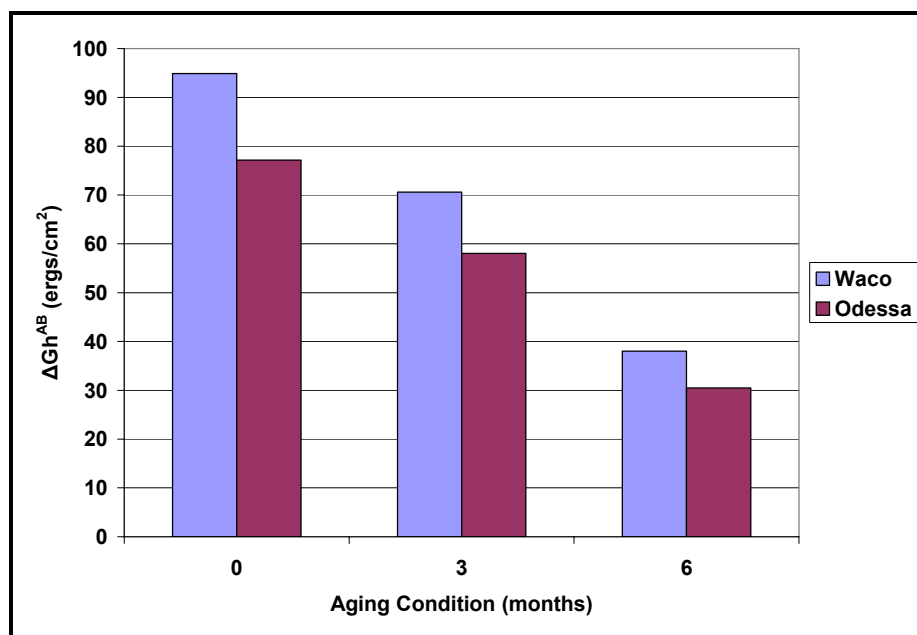
Figure 4.10 Waco and Odessa ΔG_h^{AB} with Aging

Figures 4.11, 4.12, and 4.13 indicate that the Quartzite mixture is better than the Sandstone mixture. Its adhesive bond strength attributes were superior to the Sandstone mixture in all aging conditions.
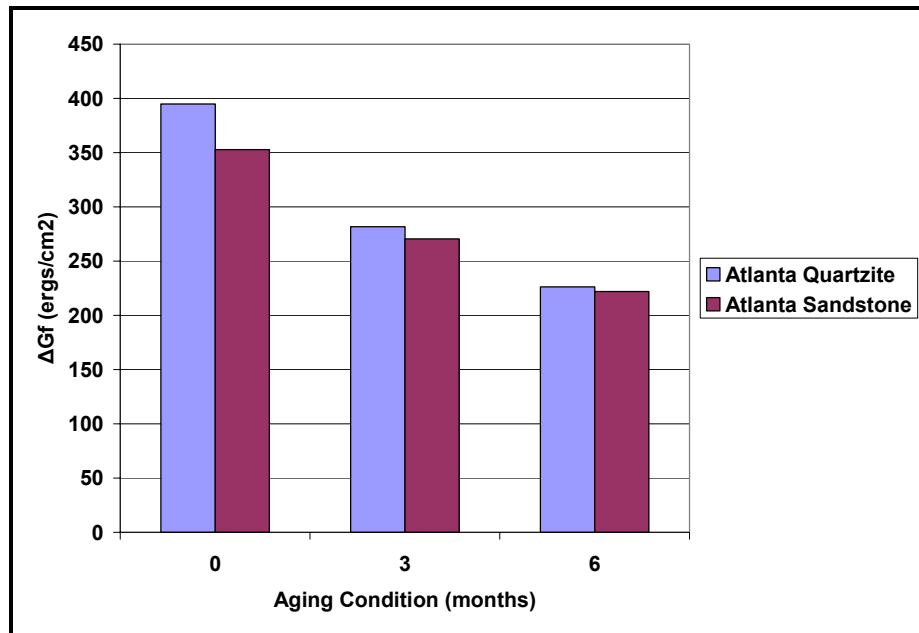
Figure 4.11 Atlanta Sandstone and Quartzite ΔG_f with Aging
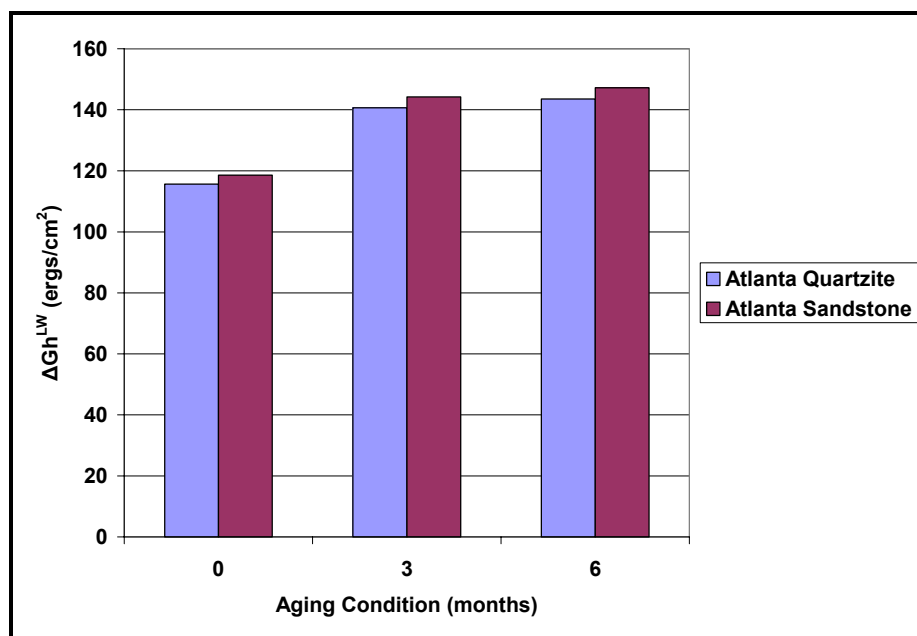
Figure 4.12 Atlanta Sandstone and Quartzite ΔG_h^{LW} with Aging
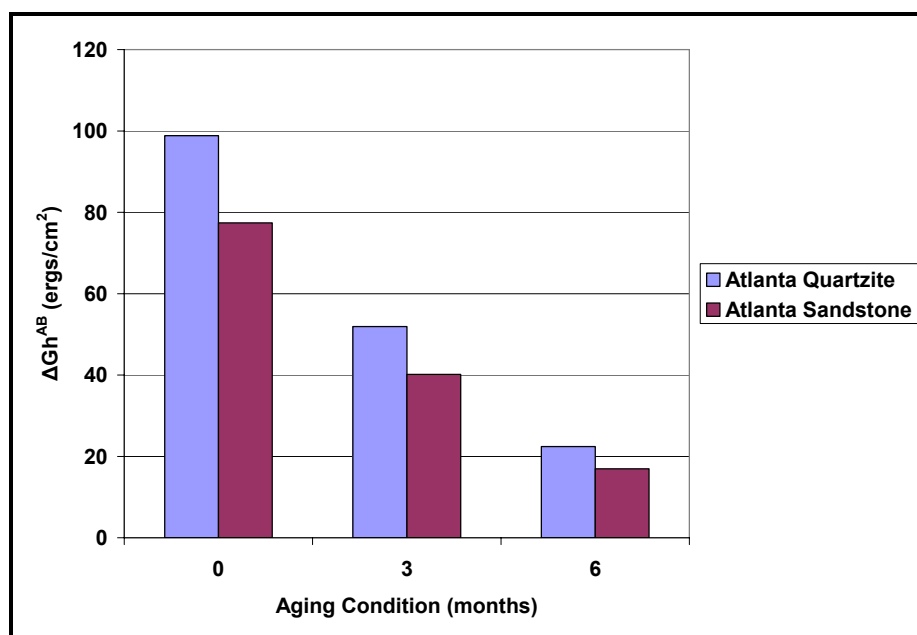
Figure 4.13 Atlanta Sandstone and Quartzite ΔG_h^{AB}

CMSE TEST RESULTS

HMAC TS Results

The tensile strength results for the HMAC mixtures are shown in Tables 4.4, 4.5, and 4.6. These Tables contain the two parameters determined during the test: σ_t and ε_f. In all cases it can be seen that as the HMAC mixture ages, σ_t increases in magnitude while ε_f decreases. This is indicative of the fact that when HMAC ages, it hardens and becomes brittle and thus breaks more easily at lower ε_f values under tensile loading. The increase in σ_t with aging is indicative of the fact that as the HMAC ages, it becomes stiffer and thus is able to carry a greater load prior to failure at lower strains.

In comparison, from Table 4.4, MnROAD 02 exhibited larger σ_t than MnROAD 02, with a reverse trend for ε_f This stems from the fact that MnROAD 02 includes a stiffer PG 58-40 asphalt.

Table 4.4 MnROAD 01 and 02 TS Results

Mixture	Aging Condition (months)	σ_t(kPa)	ε_f (microstrain)
MnROAD 01	0	235	4698
	3	372	2246
	6	475	1589
MnROAD 02	0	265	2066
	3	422	981
	6	629	675

In Table 4.5, the Waco mixture exhibited greater σ_t and lower ε_f compared to that of the Odessa mixture in all three aging conditions. In this case, since both HMAC mixtures used the same PG 70-22 asphalt, the reason for the difference is related to the

asphalt content, the aggregate type, the aggregate gradation or a combination of these factors. Aggregate surface texture may also contribute to mixture tensile strength. As shown in Figure 4.1, the surface texture as measured by AIMS shows a higher value for Odessa as compared to Waco. Mixture tensile strength also increases for dense aggregate gradations compared to open gradations. The gradations also show that the Waco aggregates are denser graded than the Odessa aggregates and the Odessa mixture had a higher asphalt content than the Waco mixture. In summary, the larger σ_t in the Waco mixture can be related to the dense gradation whereas the higher asphalt content in the Odessa can explain its higher ε_f.

Table 4.5 Waco and Odessa TS Results

Mixture	Aging Condition (months)	σ_t(kPa)	ε_f (microstrain)
	0	679	3562
Waco	3	1034	2090
	6	1527	1761
	0	363	6873
Odessa	3	756	3903
	6	944	2157

Table 4.6 shows the TS results for Atlanta Sandstone and Quartzite. In this case also the PG grade of the asphalt used in both mixtures was the same. From Table 4.6, Atlanta Quartzite has slightly greater σ_t values for all three aging conditions compared to that of Atlanta Sandstone. A distinct trend is not seen with the ε_f. Utility Theory is applied in Chapter V to provide an explanation of the contribution of the geometric properties of the aggregates to these HMAC mixture properties measured in the TS test.

Table 4.6 Atlanta Sandstone and Quartzite TS Results

Mixture	Aging Condition (months)	σ_t(kPa)	ε_f (microstrain)
Atlanta Sandstone	0	637	2964
	3	937	1381
	6	1555	1350
Atlanta Quartzite	0	837	3565
	3	1007	1307
	6	1550	935

HMAC RM Test Results

The RM test results were normalized to 20ºC for comparison with all other tests. The RM results in tension are presented in Figures 4.14 to 4.19. In all cases, as the HMAC ages, the mixture stiffens (E_t increases) and its ability to relax (m_t) reduces. In theory, the greater the m_t value, the greater the potential to resist fracture damage. Thus it follows that as the mixture ages, its potential to resist fracture damage reduces. The increase in E_t is a result of asphalt stiffening and hardening due to oxidative aging. The results are presented in a trend line developed by using a sum of errors approach to reduce the errors between the measured values and that predicted by the power law given in Equation 4.1.

$$E(t) = E_t t^{-m_t} ....(4.1)$$

$E(t)$ – time dependent elastic modulus

E_t – Relaxation modulus (tension)

t – reduced time(s)

m_t – time dependent relaxation rate

In Figures 4.14 and 4.15 MnROAD 02 exhibits a larger E_t than MnROAD 01 at 0 months aging. However, as the mixture is ages, the stiffness values equalize. This

suggests that the softer PG 58-34 binder used in MnROAD 01 has a greater susceptibility to aging and thus stiffens considerably. The change in the stress relaxation rate, m_t, in both mixtures is consistent with aging. MnROAD 02 has greater m_t values in both aging conditions, indicating that it has a greater potential to resist fracture damage compared to MnROAD 01.   Thus MnROAD 01 is expected to perform better in fatigue cracking resistance consistent with the theoretical expectation that a softer mixture exhibits longer fatigue life. Due to problems encountered during testing of the MnROAD mixtures, the RM tests were conducted only for 0 and 3 months aging conditions.
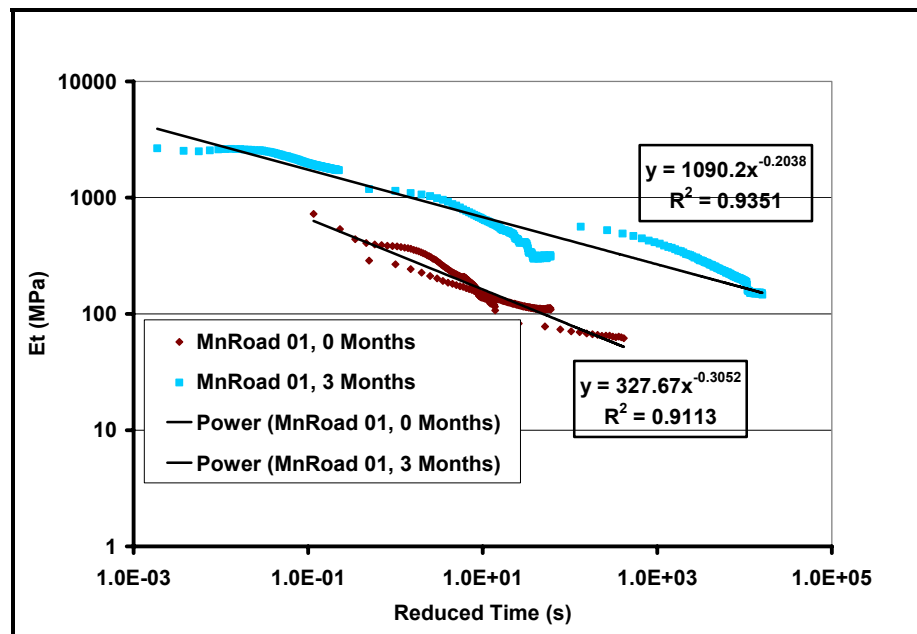
Figure 4.14 MnROAD 01 RM Results at 20°C
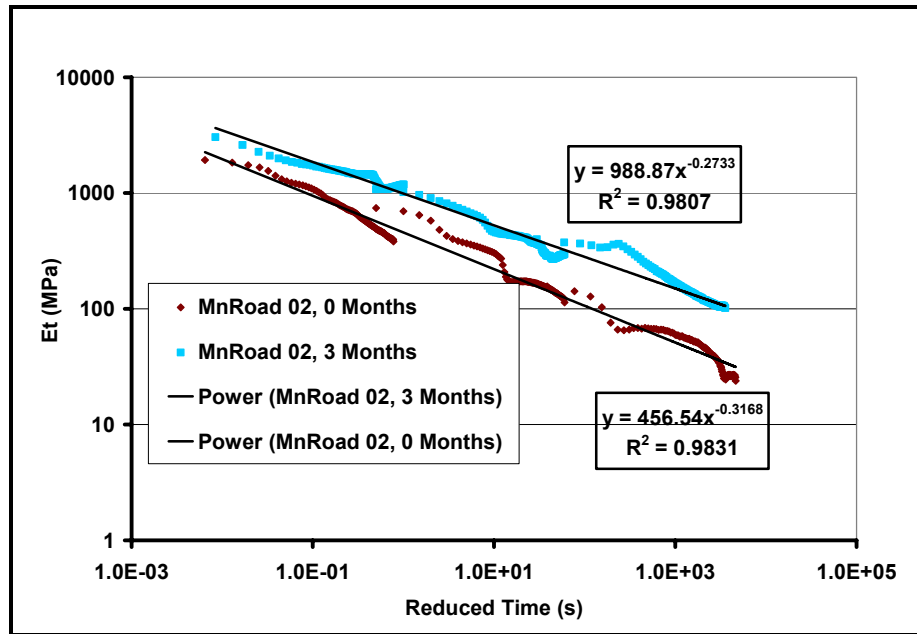
Figure 4.15 MnROAD 02 RM Results at 20°C

The Waco and Odessa mixture RM results are shown in Figures 4.16 and 4.17 Though there are marginal changes in the E_t values as the mixture ages, the m_t values are considerably different. The Waco mixture has a greater ability to relax at all three aging conditions compared to the Odessa mixture.
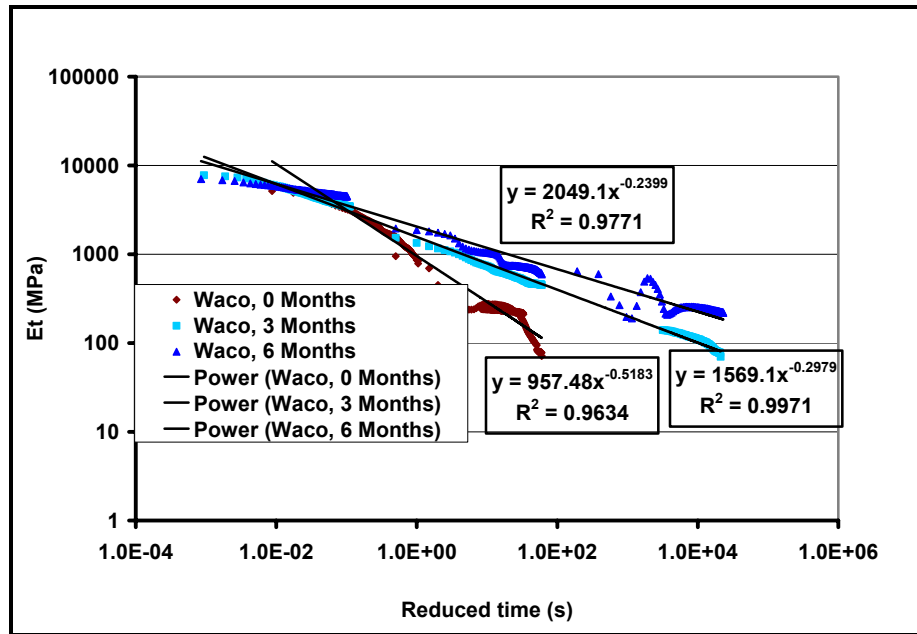
Figure 4.16 Waco RM Results at 20°C
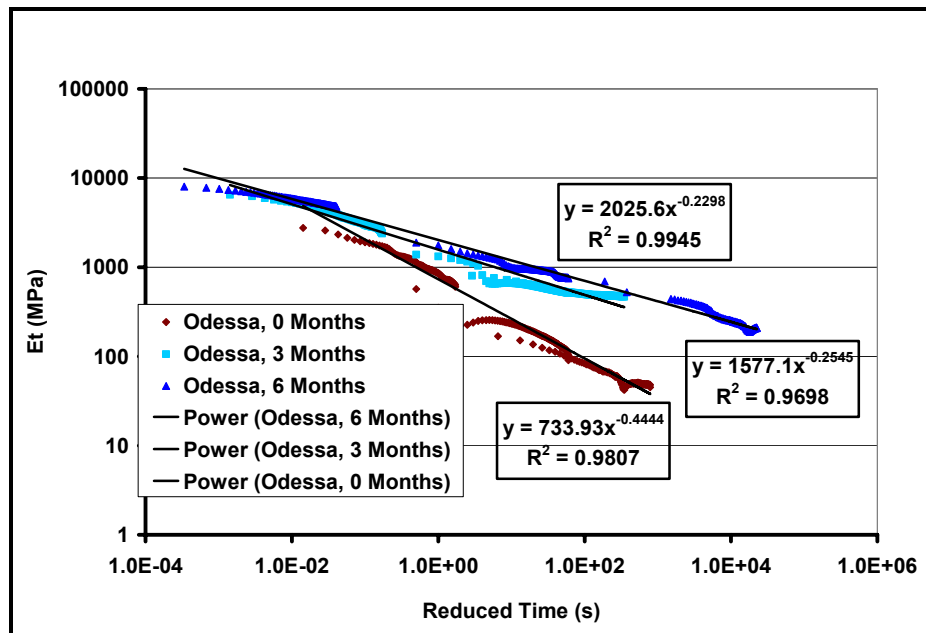
Figure 4.17 Odessa RM Results at 20°C

The Atlanta Quartzite has greater E_t and m_t values compared to Atlanta Sandstone at the 0 and 3 months aging conditions as seen in Figures 4.18 and 4.19. A reverse trend is seen for the m_t results at 6 months aging. The higher RM parameters indicate that the Atlanta Quartzite mixture is expected to exhibit a better fatigue performance compared to the Atlanta Sandstone mixture.
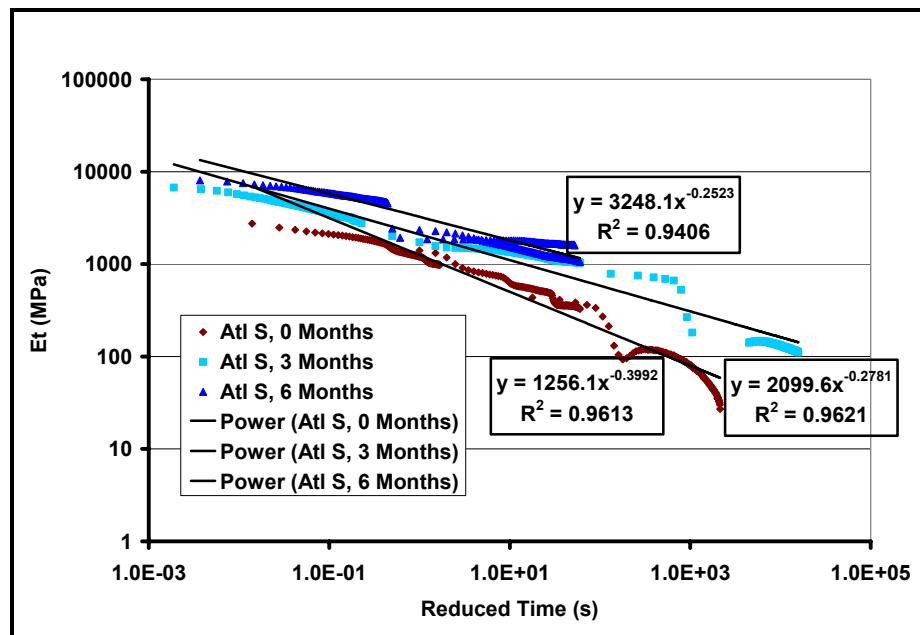
Figure 4.18 Atlanta Sandstone RM Results at 20ºC
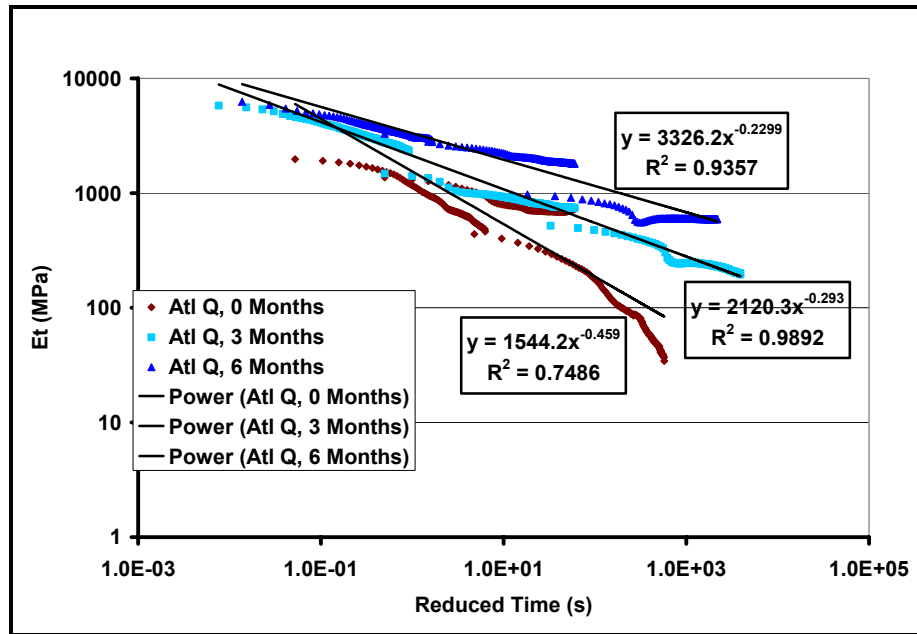
Figure 4.19 Atlanta Quartzite RM Results at 20°C

HMAC RDT Test Results

After data reduction and synthesis using the equations described in Walubita (2006), the slope (b) of the DPSE versus Log N (number of load cycles) was obtained for each aging condition and mixture. The results are shown in Figures 4.20 to 4.24. This slope indicates the rate of DPSE damage accumulation in the HMAC mixture with repeated loading. For better fatigue performance, a lower b value is required. As the HMAC mixtures age, the b values increase indicating higher susceptibility to damage accumulation.

In Figure 4.20, the plots for MnROAD 01 and MnROAD 02 at 0 months aging condition are shown. The aged MnROAD specimens could not sustain the load cycles in the RDT test, and thus the results are not presented. MnROAD 02 had a lower b value compare to MnROAD 01 indicating a better resistance to damage accumulation.
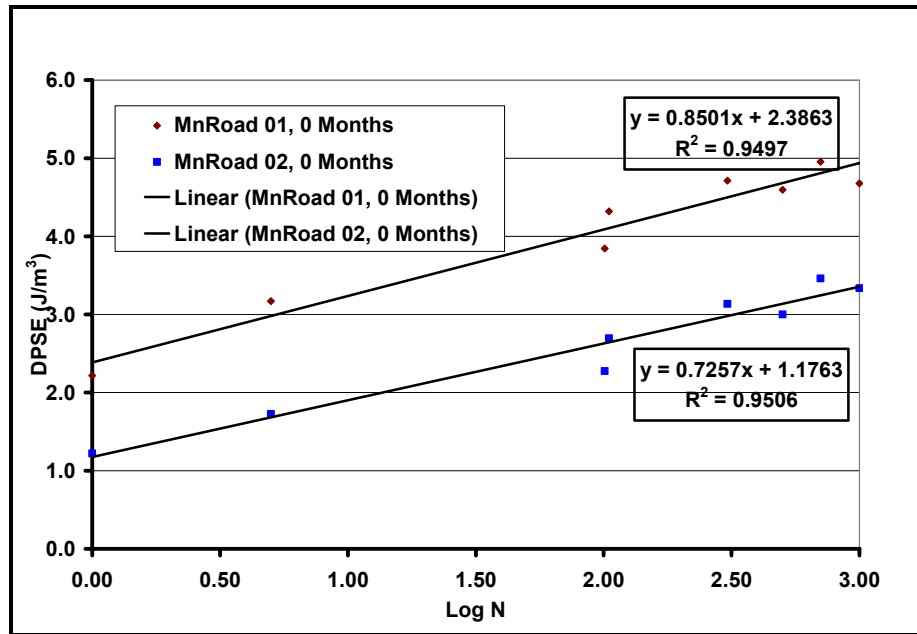
Figure 4.20 MnROAD 01 and 02 DPSE versus Log N at 20ºC

The plots in Figures 4.21 and 4.22 do not indicate a clear distinction between the Waco and Odessa mixtures. Whereas the b value at 0 months aging is lower for the Waco mixture as compared to the Odessa mixture, the reverse is seen at 3 months. At 6 months, the Waco mixture again exhibits a lower (b) than the Odessa mixture. In summary, the (b) in all cases increases with aging consistent with theoretical expectations. As HMAC mixtures age, they become more susceptible to fracture and thus exhibit higher b values.
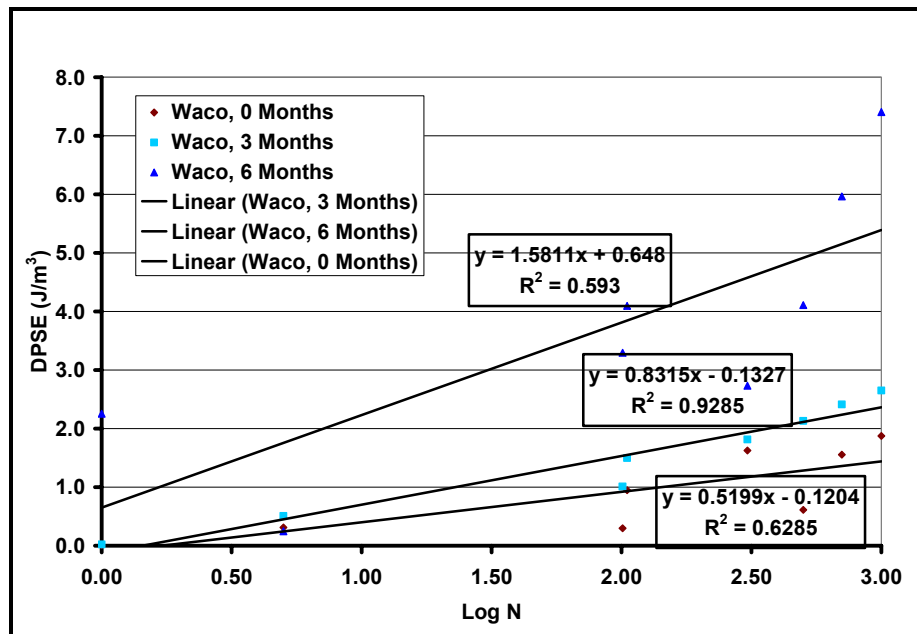
Figure 4.21 Waco DPSE versus Log N at 20ºC
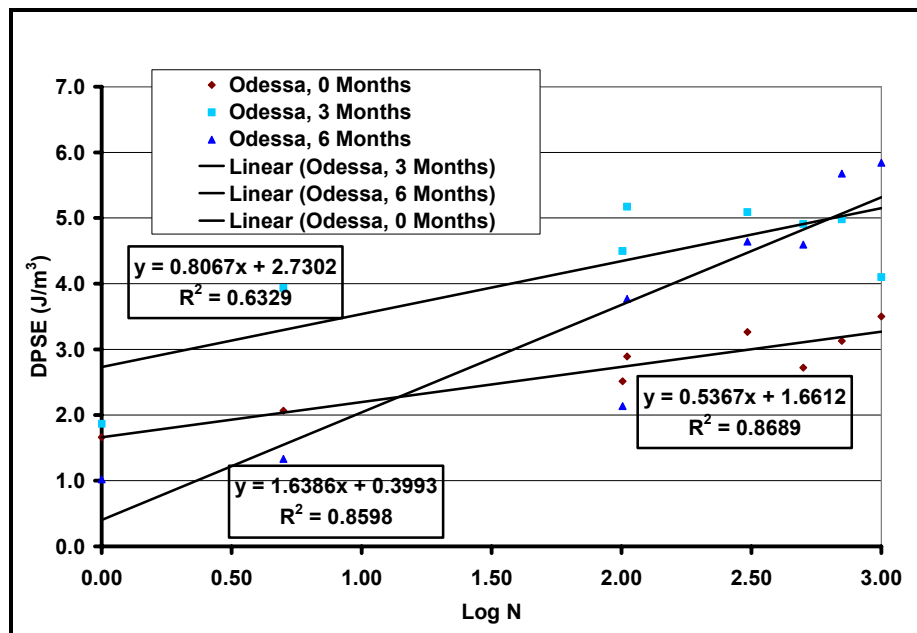
Figure 4.22 Odessa DPSE versus Log N at 20ºC

In the case of Atlanta Sandstone and Quartzite shown in Figures 4.23 and 4.24, the former exhibits higher b values than the latter. This trend continues for all aging conditions. In these two mixtures the only variation is the aggregate type, and this factor should explain the trend. Based on Figures 4.2, 4.3, and 4.4, Sandstone has higher angularity and sphericity indices. Again, Utility Theory is used in Chapter V to explain the contribution of aggregate geometric properties to the RDT test results.
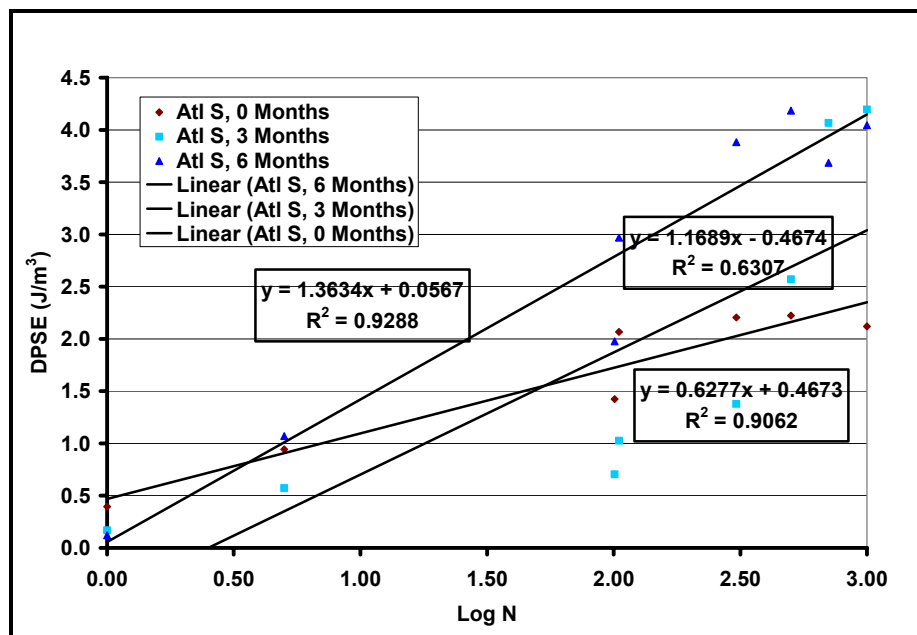
Figure 4.23 Atlanta Sandstone DPSE versus Log N at 20°C
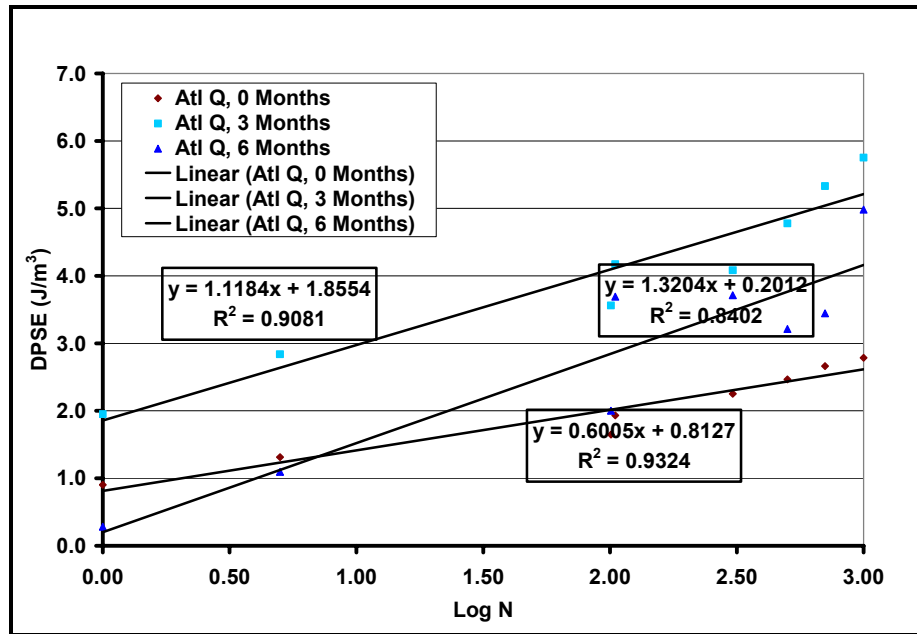
Figure 4.24 Atlanta Quartzite DPSE versus Log N at 20°C

SUMMARY

This chapter presents the laboratory test results and explains the trends in the results, including the effects of aging. Results included AIMS aggregate geometric property indices, bond strengths based on surface energy components, and HMAC mixture properties.

In general, ΔG_h^{LW} increased with aging whereas ΔG_h^{AB} and ΔG_f decreased with aging. In the TS test, an increase in σ_t was observed with an increase in oxidative aging. ε_f showed a decreasing trend with aging. In the case of the RM test, an increase in oxidative aging caused a corresponding increase in E_t and a decrease in m_t. In the RDT rest, b increased with aging.

The complete set of HMAC mixture test results is shown in appendix C.

CHAPTER V

DISCUSSION OF RESULTS

INTRODUCTION

This chapter presents the HMAC Lab and Field N_f (number of cycles to fatigue failure) for the six HMAC mixtures at the three oxidative aging conditions. Utility theory is used in an attempt to determine the contribution of aggregate geometric properties to HMAC mixture properties of the Atlanta Sandstone and Atlanta Quartzite mixtures.

LOAD CYCLES TO CRACK INITIATION (N_i)

N_i indicates the number of load cycles to initiate a crack size of 7.5mm in length in the HAMC layer, and typical results are shown in Table 5.1. The Paris' Law Fracture coefficients A and n calculated for the different HMAC mixtures for each aging condition are shown in Table 5.2. and 5.3, respectively. These material properties indicate the susceptibility of the HMAC mixture to fracture damage under loading.

Table 5.1 Typical N_i Values for the HMAC Mixtures

Parameter	Mixture	Aging Condition at 60°C ER		
		0 months	3 months	6 months
N_i	MnROAD 01	7.08E+02	N/A	N/A
	MnROAD 02	5.63E+02	N/A	N/A
	Waco	71.3E+02	1.17E+04	2.80E+04
	Odessa	1.09E+02	7.18E+04	1.52E+04
	Sandstone	53.3E+03	5.99E+03	2.48E+04
	Quartzite	23.6E+03	5.54E+03	8.10E+04

Table 5.2 Paris' Law Fracture Coefficient (*A*) for HMAC Mixtures

Parameter	Mixture	Aging Condition at 60°C ER		
		0 months	3 months	6 months
A	MnROAD 01	1.01E-06	N/A	N/A
	MnROAD 02	1.15E-06	N/A	N/A
	Waco	5.35E-07	6.63E-08	1.91E-08
	Odessa	9.94E-07	7.54E-08	4.39E-08
	Sandstone	2.87E-07	7.34E-08	2.75E-08
	Quartzite	2.66E-07	6.84E-08	2.12E-08

Table 5.3 Paris' Law Fracture Coefficient (*n*) for HMAC Mixtures

Parameter	Mixture	Aging Condition at 60°C ER		
		0 months	3 months	6 months
n	MnROAD 01	3.33	N/A	N/A
	MnROAD 02	3.13	N/A	N/A
	Waco	1.92	3.33	4.17
	Odessa	2.27	4.00	4.35
	Sandstone	2.50	3.57	4.00
	Quartzite	2.17	3.45	4.35

LOAD CYCLES TO CRACK PROPAGATION N_p

N_p indicates the number of load cycles to propagate a crack of 7.5mm length through the HMAC layer. The equations for its determination as described in Chapter III are dependent on the pavement thickness (d), *A* and *n*, and the design shear strain (γ). These inputs were used to calculate the values shown in Table 5.4.

Table 5.4 Typical N_p Values for HMAC Mixtures

Parameter	Mixture	Aging Condition at 60°C ER		
		0 months	3 months	6 months
N_p	MnROAD 01	9.41E+07	N/A	N/A
	MnROAD 02	2.54E+07	N/A	N/A
	Waco	1.11E+07	7.75E+06	4.44E+06
	Odessa	8.39E+06	3.82E+06	1.67E+06
	Sandstone	6.99E+06	2.01E+06	5.82E+05
	Quartzite	6.48E+06	2.41E+06	4.03E+05

STATISTICAL ANALYSIS OF Lab N_f RESULTS

The CMSE approach utilizes a 95% reliability prediction factor, so a statistical analysis of the test results was done to determine the precision and variability of the results. Three sets of measured HMAC mixture properties needed to predict Lab N_f were used: σ_t, E_t and m_t, and b. These parameters were determined for at least two replicate samples, and a one sample t-test was performed. Eight Lab N_f predictions were determined based on the combination of the three sets of HMAC mixture parameters and two replicate specimens. Note that the Lab N_f values were computed as the sum of N_i and N_p without multiplying with any shift factors. The combination of HMAC mixture properties used in the statistical analysis is shown in Table 5.5.

Table 5.5 HMAC Mixture Property Combinations for Statistical Analysis

ID	HMAC Mixture Property Combination	Lab N_f	Ln Lab N_f
1	σ_{t1}; (E_{t1}, m_{t1}); b_1	N_{f1}	Ln N_{f1}
2	σ_{t1}; (E_{t1}, m_{t1}); b_2	N_{f2}	Ln N_{f2}
3	σ_{t1}; (E_{t2}, m_{t2}); b_1	N_{f3}	Ln N_{f3}
4	σ_{t1}; (E_{t2}, m_{t2}); b_2	N_{f4}	Ln N_{f4}
5	σ_{t2}; (E_{t1}, m_{t1}); b_1	N_{f5}	Ln N_{f5}
6	σ_{t2}; (E_{t1}, m_{t1}); b_2	N_{f6}	Ln N_{f6}
7	σ_{t2}; (E_{t2}, m_{t2}); b_1	N_{f7}	Ln N_{f7}
8	σ_{t2}; (E_{t2}, m_{t2}); b_2	N_{f8}	Ln N_{f8}
Mean Ln Lab N_f			$\bar{x}$
Stdev			σ
COV (%)			$\dfrac{100\sigma}{\bar{x}}$
95% CI			$\bar{x} \pm t_{\frac{\alpha}{2}, n-1}\left(\dfrac{\sigma}{\sqrt{n}}\right)$

The 0 months Lab N_f mean values determined from the statistical analysis at 95% reliability level are shown in Table 5.6. Generally there was a decrease in N_f with aging. Figure 5.1 shows a comparison of the Lab N_f of MnROAD 01 and 02 which were tested only at the 0 months aging condition. Figure 5.2 shows Lab N_f values for the Texas HMAC tested in this study. Table 5.7 shows the coefficients of variation (COV) for the mean Lab N_f. A range for the COV of 0.19% to 3.87% was deemed statistically adequate. Appendix D shows the complete Lab N_f values for all six mixtures at the different aging conditions.

Table 5.6 Mean Lab N_f for HMAC Mixtures

Parameter	Mixture	Aging Condition at 60°C ER		
		0 months	3 months	6 months
Mean Lab N_f	MnROAD 01	5.98E+07	N/A	N/A
	MnROAD 02	1.84E+07	N/A	N/A
	Waco	1.82E+07	7.19E+06	4.05E+06
	Odessa	1.07E+07	3.74E+06	1.71E+06
	Sandstone	5.44E+06	2.41E+06	5.99E+05
	Quartzite	1.04E+07	1.49E+06	6.50E+05

Table 5.7 Percent Coefficient of Variation (COV) for the Mean Lab N_f

Aging Condition (months)	HMAC Mixtures					
	MnROAD 01	MnROAD 02	Waco	Odessa	Atlanta Sandstone	Atlanta Quartzite
0	0.95	3.87	3.57	1.91	3.52	3.11
3	N/A	N/A	0.58	2.42	0.98	3.72
6			1.74	0.19	1.03	1.79
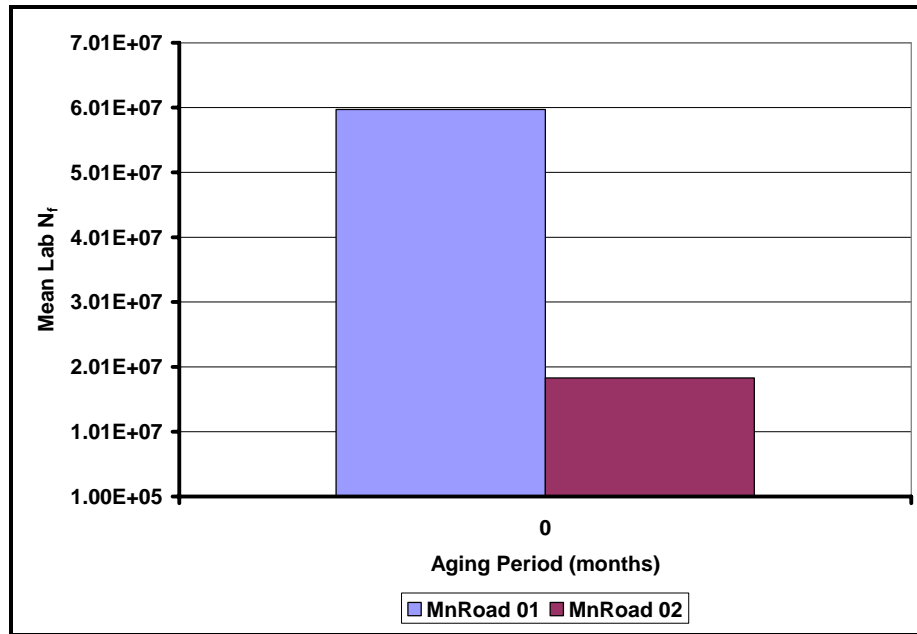
Figure 5.1 Lab N_f for MnROAD 01 and 02
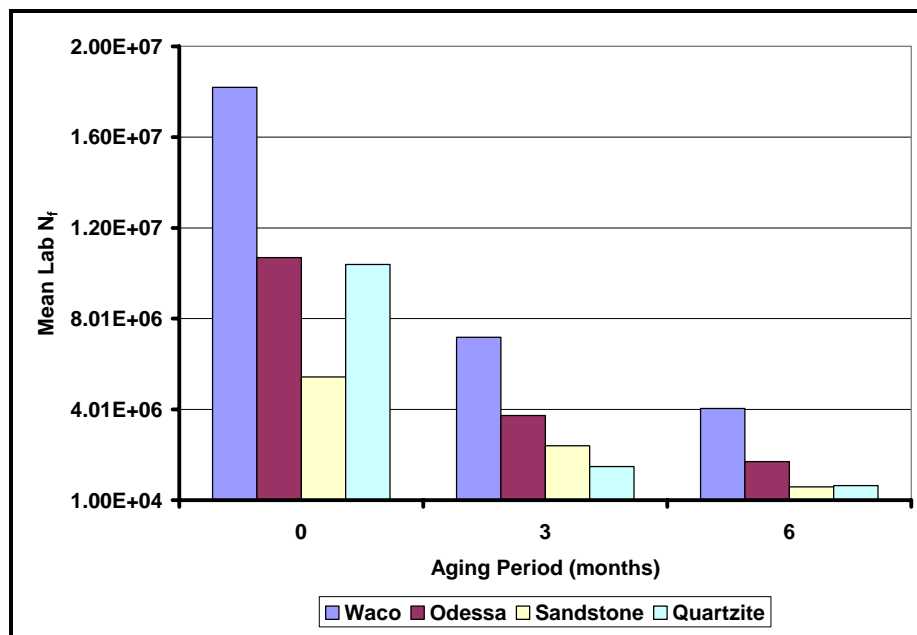
Figure 5.2 Lab N_f versus Aging for Texas HMAC Mixtures

FIELD HMAC N_f

In predicting the Field N_f of the HMAC mixtures, three shift factors were taken into consideration. SF_a, SF_h, and SF_{ag} were used to account for the effects of anisotropy, healing of micro cracks, and field aging of the HMAC respectively. Equations 3.3 and 3.4 are used to estimate SF_a and SH_h. To account for field aging in the HMAC, a methodology proposed in Walubita (2006) was used to develop SF_{ag}. SAFT and Pressure Aging Vessel (PAV) procedures were used to age asphalt binders and DSR function for asphalt binder subjected to the three aging conditions, SAFT, SAFT + PAV* 16hrs, and SAFT + PAV* 32hrs was used to determine SF_{ag}. Table 5.8 presents the SF_{ag} as a function of pavement age for the asphalt binders used in this study. Note that PG 76-22 results are the same as that in Walubita (2006).

Table 5.8 SF_{ag} Values for Asphalt Binders

Pavement Age (Years)	SFag			
	PG 58-34	PG 58-40	PG 70-22	PG 76-22
0	1.000	1.000	1.000	1.000
2	0.189	0.160	0.272	0.303
6	0.094	0.098	0.163	0.221
12	0.032	0.033	0.072	0.109
18	0.019	0.020	0.049	0.081
20	0.017	0.018	0.044	0.070

Field N_f is then estimated as in Equation 5.1. Table 5.9 shows the Field N_f values at year 20 the design life of the pavement.

$$\text{Field } N_f = SF_a \times SF_h \times SF_{ag} \times \text{Lab } N_f \dots\dots\dots\dots\dots\dots\dots\dots\dots\dots\dots\dots\dots\dots\dots\dots\dots(5.1)$$

Table 5.9 Mean Field N_f Values at Year 20

Mixture	Mean Field Nf @ Year 20
MnROAD 01	1.37E+07
MnROAD 02	4.46E+06
Waco	1.08E+07
Odessa	6.34E+06
Sandstone	5.13E+06
Quartzite	9.80E+06

DISCUSSION OF N_f RESULTS

Based on Figure 5.2 there is a general decline in HMAC fatigue life with aging. The rate of decline of N_f is dependent on how the fundamental HMAC mixture properties change with oxidative aging.

Table 5.6 indicates an interesting trend that agrees with theoretical expectations that the softer the asphalt, the better its resistance to fatigue cracking. MnROAD 01 performed better than MnROAD 02, since the latter included a softer PG 58-34 asphalt as compared to the stiffer PG 58-40 asphalt in the latter. Likewise,Odessa and Waco which used softer PG 70-22 asphalt performed better in fatigue resistance as compared to Atlanta Sandstone and Quartzite which utilized stiffer PG 76-22 asphalt. All these asphalts used SBS modifier, and therefore there was no distinction with respect to the type of modifier used in the asphalt.

The Waco HMAC mixture performed better in fatigue resistance compared to the Odessa mixture. The reasons for this difference in performance can be attributed to many variables including asphalt binder content, asphalt film thickness, aggregate structure, stiffness indicated by RM parameters and the accumulation of DPSE. Theoretically it is expected that the higher the asphalt content, the thicker the film thickness and

consequently the greater resistance to oxidative aging and susceptibility to cracking. In this case, this was not observed since the Odessa HMAC mixture had a higher asphalt content compared to the Waco HMAC mixture. A reasonable explanation for the greater resistance to fatigue cracking exhibited by the Waco HMAC mixture, therefore, can be attributed to its higher adhesive bond energies compared to the Odessa HMAC mixture, implying that the aggregate had greater affinity and compatibility with the PG 70-22 binder. This may also have been the reason for the corresponding higher fundamental material properties of the Waco HMAC mixture compared to the Odessa HMAC mixture. The steeper decline of fatigue resistance of the Odessa HMAC mixture indicates a greater susceptibility to oxidative aging that leads to brittleness and eventual cracking.

A consistent trend was not observed between the results obtained from the Atlanta Sandstone and Quartzite mixtures. At 0 and 6 months aging conditions, the Atlanta Quartzite mixture exhibited a higher fatigue resistance compared to the Atlanta Sandstone mixture, and a reverse trend was observed at the 3 months aging condition. The rates of N_f decline were also not significantly different. The only reasonable explanation for the inconsistent fatigue performance is that the various mixture and aggregate properties interact and compensate for each other such that the end result is not significantly different.

THE EFFECT OF AGGREGATE GEOMETRIC PROPERTIES

The inconsistent trend observed in the Lab N_f values for Atlanta Quartzite and Sandstone HMAC mixtures warranted further investigation. Utility Theory given in equation 5.2 was used to assess the contribution of four aggregate geometric properties

which have been identified in the literature as important with respect to fatigue cracking in HMAC.

$$U_x = \sum w_i \times q_i \dotfill (5.2)$$

U_x - overall utility for aggregate type x

w_i – weight for geometric property i

q_i – aggregate geometric property i for aggregate x

These geometric properties were evaluated for their effects on the three sets of HMAC mixture properties: σ_t, E_t and m_t and b. Weights according to the contribution of each geometric property to the HMAC mixture property were given and used in the computation of the overall utilities for the aggregate type in question. The aggregate geometric property indices measured with AIMS were used in the derivation of these utilities. A higher utility indicated a greater contribution of the aggregate geometric properties to the HMAC mixture property

For σ_t and the RM parameters, surface texture was given a weight of 0.5, gradient angularity and sphericity were both given weights of 0.2 and 2D Form was given a weight of 0.1 based on the discretion of the author as to the influence of these properties on fatigue. For the b value obtained in the RDT test, surface texture was given a weight of 0.2, gradient angularity was assigned 0.4, 0.3 was assigned for sphericity and 0.1 was assigned for 2D Form according to how these factors were perceived to affect the accumulation of DPSE damage by the formation of micro cracks. Table 5.10 indicates the computed utilities.

Table 5.10 Utility Theory Results for the Contribution of Aggregate Geometric

Properties to HMAC Properties

Aggregate Geometric Property	w_i	Atlanta Quartzite		Atlanta Sandstone		Upper Limit of x_i
		x_i	u_i	x_i	u_i	
HMAC Tensile Strength and RM Parameters						
Surface Texture	0.5	171.37	0.19	139.37	0.15	460
Gradient Angularity	0.2	2968.15	0.11	3410.19	0.13	5400
Sphericity	0.2	0.69	0.17	0.746	0.19	0.8
2D Form	0.1	8.06	0.12	8.05	0.12	6.5
		ΣU	**0.59**	ΣU	**0.59**	
b value						
Surface Texture	0.2	171.37	0.07	139.37	0.06	460
Gradient Angularity	0.4	2968.15	0.22	3410.19	0.25	5400
Sphericity	0.3	0.69	0.26	0.746	0.28	0.8
2D Form	0.1	8.06	0.12	8.05	0.12	6.5
		ΣU	**0.68**	ΣU	**0.72**	

Based on Table 5.10, the aggregate geometric properties of surface texture, gradient angularity, sphericity, and 2D Form contributed equally to the TS and RM properties of the two HMAC mixtures. In the case of the b value, however, interactions within the geometric properties were seen to play a role. A higher utility value for Atlanta Quartzite as compared to Atlanta Sandstone may explain the reason for higher b values in the Quartzite mixture, but further investigation and verification is recommended.

SUMMARY

The following points summarize the major findings in this chapter:

- The statistical variability obtained in the determination of Lab N_f was deemed acceptable. The Atlanta Quartzite HMAC mixture exhibited the least COV (1.7% to 3.11%), whereas the highest COV (1.03% to 3.52%) was seen in the Atlanta Sandstone HMAC mixture.

- A general exponential decline of N_f with aging was observed in the Texas mixtures. Waco was deemed to be the best HMAC since the N_f value after 20 years of aging exposure was still greater than the design 5×10^6 ESALS.

- Utility Theory was used to explain the effect of geometric aggregate properties on the HMAC mixture properties and ultimately N_f. The effect of a combination of geometric properties on the TS and RM parameters was equal in the Atlanta Sandstone and Quartzite HMAC mixtures. However, a distinction was found in their contribution to the b value.

CHAPTER VI

CONCLUSIONS AND RECOMMENDATIONS

The conclusions and recommendations based on the objectives of this research are presented in this chapter.

CONCLUSIONS

To validate the CMSE approach as a reliable tool to measure the fatigue resistance of selected HMAC mixtures.

- The CMSE approach which utilizes fundamental material properties such as tensile strength σ_t, relaxation modulus E_1, stress relaxation rate m_t, the rate of DPSE damage accumulation b and the adhesive fracture and healing bond strengths of the asphalt-aggregate mixture ΔG_f, ΔG_h^{LW}, and ΔG_h^{AB} was found to be an effective approach to determine fatigue resistance of HMAC. The results obtained in this study compared to those obtained in a previous study by Walubita (2006).

- The CMSE approach utilizes test protocols which represent actual field HMAC conditions including anisotropy, healing, crack initiation, crack propagation and the effects of binder oxidative aging. The approach validated the theoretical concept of HMAC fatigue life decline with oxidative aging.

To evaluate and compare the fatigue resistance of selected HMAC mixtures that vary in terms of mixture type, aggregate geometric properties, and binder type.

Mixture Type

- The Waco mixture which used a Superpave_19mm aggregate structure with a PG 70-22 asphalt binder performed better in terms of fatigue resistance compared to the Odessa mixture which used a CMHB_F aggregate structure.

- The asphalt content of 7.3% in the Odessa mixture ensured thicker film thicknesses on the aggregates compared to the 5.3% asphalt content in the Waco mixture. This ensured that the Odessa mixture had higher failure strains in all aging conditions compared to the Waco mixture.

Aggregate Properties

- In this study, the measured aggregate properties did not influence the TS and RM test parameters. However a contribution of the geometric properties was seen to affect the b value from the RDT test using Utility Theory.

Binder Type

- Based on the MnROAD 01 and 02 mixtures, the softer the asphalt binder with all other components such as gradation, asphalt content, aggregate type remaining the same, the better the HMAC mixture performs in terms of fatigue resistance.

To evaluate and quantify the influence of other factors such as aggregate geometric properties or aggregate structure type on the fatigue resistance of the selected HMAC mixtures.

- The use of Utility Theory revealed the possible effects of aggregate geometric properties on the HMAC mixture properties and consequently on their fatigue resistance.

RECOMMENDATIONS

- The effect of aggregate geometric properties on the fatigue resistance of HMAC mixtures needs to be further validated. This could be done with the use of the same aggregate type and gradation with and without crushing, for example, to evaluate the effects of angularity.

- The hypothesis that stiffening the asphalt binder improves rutting as well as fatigue resistance needs to be investigated further since contradictory evidence was found in this study based on the results of the MnROAD 01 and 02 mixtures.

- The effect of water which is also a detrimental factor on pavement performance should also be looked at and incorporated into a fatigue design and analysis system.

REFERENCES

Aglan, H., Othman, L., Figueroa, L., Rollings, R., (1993). "Effect of styrene-butadiene-styrene block copolymer on fatigue crack behavior of asphalt concrete mixtures." *Transportation Research Record 1417,* Transportation Research Board, Washington D.C., 178-186.

Alrousan, T. M. (2004). "Characterization of aggregate shape properties using a computer automated system." Ph.D. dissertation, Texas A&M Univ., College Station, Texas.

American Association of State Highway and Transportation Officials, (AASHTO). (2003). "Standard method of test for determining dynamic modulus of hot mix asphalt concrete mixtures, TP 62-03." Washington D.C.

American Association of State Highway and Transportation Officials, (AASHTO). (2000). "Standard method of test for bulk specific gravity of compacted bituminous mixtures using saturated surface dry specimens, T 166-00." Washington D.C.

American Association of State Highway and Transportation Officials, (AASHTO). (1998). "Standard test method for determining the rheological properties of asphalt binder using a dynamic shear rheometer, TP5-98." Washington D.C.

American Association of State Highway and Transportation Officials, (AASHTO). (1996). "Standard practice for grading or verifying the performance grade of an asphalt binder, PP6-94." Washington D.C.

American Association of State Highway and Transportation Officials, (AASHTO). (1994). "Standard practice for short and long term aging of hot mix asphalt, PP2." *AASHTO Provisional Standards*, Washington D.C.

American Association of State Highway and Transportation Officials, (AASHTO). (1993). "Standard practice for bulk specific gravity of compacted bituminous mixtures using saturated surface dry specimens, PP19." *AASHTO Provisional standards*. Washington D.C.

Bathina, M. (2005). "Quality analysis of the aggregate imaging system (AIMS) Measurements." M.S. thesis, Texas A&M Univ., College Station, Texas.

Bell, C. A., (1990). "Relationship between laboratory aging tests and field performance of asphalt-concrete mixtures." *Proc., Serviceability and Durability of Construction Materials*, 13620, 745-754.

Bhasin, A. (2006). "Development of methods to quantify bitumen-aggregate adhesion and loss of adhesion due to water" Ph.D. dissertation, Texas A&M Univ., College Station, Texas.

Brule B. (1996). "Polymer-modified asphalt cements used in the road construction industry: basic principles." *Transportation Research Record 1535,* Transportation Research Board, Washington D.C., 48-53.

Chen, J. S., Liao, M. C., (2002). "Evaluation of internal resistance in hot-mix asphalt (HMA) concrete." *Construction and Building Materials*, 16(6), 313 – 319.

Cheng, D. (2002). "Surface free energy of asphalt-aggregate system and performance analysis of asphalt concrete based on surface energy." Ph.D. dissertation, Texas A&M Univ., College Station, Texas.

Dongre, R., Button, J. W., Klutz, R. Q., Anderson, D. A., (1997). "Evaluation of superpave binder specification with performance of polymer-modified asphalt pavements." *Progress of Superpave (Superior Performing Asphalt Pavement): Evaluation and Implementation*, ASTM STP 1332, R. N. Jester, Ed., American Society for Testing and Materials, West Conshohocken, Pennsylvania, 80-100.

Epps, J. A., Monismith, C. L. (1972). "Fatigue of asphalt concrete mixtures – summary of existing information." *Fatigue of Compacted Bituminous Aggregate Mixtures*, ASTM STP 508, American Society for Testing and Materials, West Conshohocken, Pennsylvania, 19 – 45.

Fletcher, T., Chandan, C., Masad, E., Krishna, S., (2003). "Aggregate imaging system for characterizing the shape of fine and coarse aggregates." *Transportation Research Record 2174*, Transportation Research Board, Washington D.C., 67-77.

Freeman, T. (2004). "Flexible pavement database." Research Project 187-06, Texas Transportation Institute, College Station, Texas.

Glover, C. J., Davison, R. R., Domke, C. H., Ruan, Y., Juristyarini, P., Knorr, D.B., and Jung, H.S. (2005). "Development of a new method for assessing asphalt binder durability with field validation." Report FHWA/TX-03/1872-2, Texas Transportation Institute, College Station, Texas.

Goulias, D. G., (2001). "Durability evaluation of asphalt mixtures modified with recycled tire rubber." *Journal of Solid Waste Technology and Management*, 27 (3), 169-171.

Hand, A. J., Stiady, J. L., White, T. D., (2001). "Gradation effects on hot-mix asphalt performance." *Transportation Research Record 1767*, Transportation Research Board, Washington D.C., 152-157.

Huang, E. Y., Grisham, D. A. (1972). "Effect of geometric characteristics of aggregates on the fatigue response of bituminous paving mixtures." *Fatigue of Compacted Bituminous Aggregate Mixtures*, ASTM STP 508, American Society for Testing and Materials, West Conshohocken, Pennsylvania, 145 – 160.

Huang, S-C, Tia, M, T., Ruth, B. E., (1995). "Evaluation of aging characteristics of modified asphalt mixtures." *Engineering Properties of Asphalt Mixtures and the Relationship to Their Performance*, ASTM STP 1265, Gerald A. Huber and Dale S. Decker, Eds, American Society for Testing and Materials, Philadelphia.

Huang, Y. H., (2004). *Pavement analysis and design*, 2nd Edition, Pearson Education Inc., Upper Saddle River, New Jersey.

Karakouzian, M., Dunning, M. R., Dunning, R. L., Stegeman, J. D., (1996). "Performance of hot mix asphalt using coarse and skip graded aggregates." *Journal of Materials in Civil Engineering*, 8(2) 101 – 107.

Khattak, M. J., Baladi, G. Y., (2001). "Fatigue and permanent deformation models for polymer-modified asphalt mixtures." *Transportation Research Record 1767*, Transportation Research Board, Washington D.C., 135-145.

Khattak, M. J., Baladi, G. Y., (1998). "Engineering properties of polymer-modified asphalt mixtures." *Transportation Research Record 1638*, Transportation Research Board, Washington D.C., 12-22.

Kim, Y. R., Kim, N., Khosla, N. P., (1992). "Effects of aggregate type and gradation on fatigue and permanent deformation of asphalt concrete." *Effects of Aggregates and Mineral Fillers on Asphalt Mixture Performance*, ASTM STP 1147, American Society for Testing and Materials, Philadelphia.

Kuennen, T., (2005). "Polymer-modified asphalt comes of age." *Better Roads,* 75(11), 70 – 79

Lufti, R., Saboundjian, S., Minassian, G., (2001). "Field aging effects on fatigue of asphalt concrete and asphalt rubber concrete." *Transportation Research Record 1767*, Transportation Research Board, Washington D.C., 126-134.

Lytton, R. L., Uzan, J., Fernando, E.G, Roque, R., Hiltunen, D., and Stoffels, S. (1993). "Development and validation of performance prediction models and specifications for asphalt binders and paving mixes." Report SHRP-A-357, Strategic Highway Research Program, National Research Council, Washington, D.C.

Mahmoud, E. M., (2005). "Development of experimental methods for the evaluation of aggregate resistance to polishing, abrasion, and breakage" M.S. thesis, Texas A&M Univ., College Station, Texas.

Masad, E. (2001). "Review of imaging techniques for characterizing the shape of aggregates used in asphalt mixes." A Paper Presented at the 9th Annual Symposium International Center for Aggregate Research (ICAR), Austin, Texas.

Monismith, C. L., (1970). "Influence of shape, size, and surface texture on the stiffness and fatigue response of asphalt mixtures." *Highway Research Board Special Report 109*, 4 – 11.

Othman, A., Figeroa, L., Aglan, H., (1995). "Fatigue behavior of styrene-butadiene-styrene modified aspahltic mixtures exposed to low-temperature cyclic aging." *Transportation Research Record 1492,* Transportation Research Board, Washington D.C., 129-134.

Pan, T. and Tutumluer, E., (2001). "Imaging based evaluation of coarse aggregate size and shape properties affecting pavement performance." *Geotechnical Special Publication 130, Advances in Pavement Engineering,* 33-47.

Smith, R. E., M. I. Darter, Herrin, S. M., (1979). Highway pavement distress identification manual for highway condition and quality of highway construction survey, NCHRP 1 – 19; Federal Highway Administration

Walubita F. L. (2006). "Comparison of fatigue analysis approaches for predicting fatigue lives of hot mix asphalt concrete mixtures (HMAC)." Ph.D. dissertation, Texas A&M Univ., College Station, Texas.

Williamson, S. D., Gaughan, R. L., (1992). "A field evaluation of rutting and cracking in asphalt with modified binders." *Proc., 16th Australian Road Research Board Conference Part 2,* 223-235.

APPENDIX A

SURFACE ENERGY LABORATORY TESTS

THE WILHELMY PLATE METHOD

ID	Procedure
1	About 50g of asphalt binder in a tin is heated at the respective mixing temperature for the asphalt as indicated in Table 3.8 in an oven. The tin is removed from the oven after about an hour of heating and placed on a hot plate to maintain the temperature during the coating process.
2	A 24 × 50mm micro glass plate is passed for about 6 times through a blue flame of a propane torch to remove all forms of moisture before the coating process. The glass plate is then dipped to a depth of about 15mm into the tin of asphalt binder to coat the surface about 0.25mm thick. The coated glass plate is turned over and placed in a slide holder. This is then de-aired in a dessicator overnight prior to the measurement of the dynamic contact angles.
3	The coated glass slide is then automatically immersed and withdrawn from a beaker of probe liquid using the Dynamic Contact Analyzer (DCA) Microbalance. During the immersion and withdrawal process, the dynamic contact angle is measured via WinDCA software.
4	The three probe liquids used to determine the three unknown surface free energies of the asphalts, Γ^{LW}, Γ^+, and Γ^-, are glycerol, formamide, and water. These probe liquids are used because their respective surface free energies are known and they have been shown not to react with the asphalt binder.
5	The equation in 6 is used to determine the three unknown surface free energy of the asphalt binder. Three probe liquids are used because three unknown surface free energies are needed and therefore three equations of three unknown are generated and solved to determine them.
6	$$\Gamma_L\left(1+\cos\theta\right)=2\sqrt{\Gamma_L{}^{LW}\times\Gamma_b{}^{LW}}+2\sqrt{\Gamma_L{}^+\times\Gamma_b{}^-}+2\sqrt{\Gamma_L{}^-\times\Gamma_b{}^+}$$ $\Gamma_{L,b}$ – Surface Free Energy of the probe liquid (L) or asphalt binder (b) θ - dynamic contact angle measured (advancing or receding)

THE MICRO CALORIMETER METHOD

ID	Procedure
1	Size # 4 aggregates are crushed into finer particles and sieved to pass sieve #100 and retained on sieve # 200. The aggregates are washed in distilled water over sieve # 200 and oven dried.
2	About 8 grams of the aggregates is placed in a 16 ml glass vial with a polypropylene open top cap sealed with lined silicon septa. Another vial with the same sealing is kept empty and used as a reference vial. The vials are preconditioned at 150°C for 4hrs below 300 millitorr vacuum. The vacuum is achieved by the help of syringes which pierce the silicon septa and suck out the air. After preconditioning the vials are brought to testing temperature of 25°C in a water bath
3	The empty vial is placed in the reference cell of the MC and the vial with the aggregate placed in the reaction cell. 2 syringes each, filled 2 ml of probe liquid are placed on top of the vials in both cells and software with the MC records the differential heat between the two cells until equilibrium is reached in about 30 – 40 minutes. As soon as equilibrium is reached the probe liquid is injected into the vials and the enthalpy of immersion is measured throughout the test which takes about 2 hrs.
4	The three probe liquids used to determine the three unknown surface free energies of the aggregates, Γ^{LW}, Γ^{+}, and Γ^{-}, are heptane, benzene, and chloroform.
5	The equation in 6 is used to determine the three unknown surface free energy of the aggregates. Three probe liquids are used because three unknown surface free energies are needed and therefore three equations of three unknown are generated and solved to determine them.
6	$$\Delta H_{imm} - T\Delta S_{imm} = \Gamma_L - 2\sqrt{\Gamma_L^{LW} \times \Gamma_a^{LW}} - 2\sqrt{\Gamma_L^{+} \times \Gamma_a^{-}} - 2\sqrt{\Gamma_L^{-} \times \Gamma_a^{+}}$$ $\Gamma_{L,b}$ – Surface Free Energy of the probe liquid (L) or aggregate (a) ΔH_{imm} – Enthalpy of immersion ΔS_{imm} – Entropy of immersion

APPENDIX B

AIMS GEOMETRIC PROPERTY TEST RESULTS

DANNER ½" CLASS D - MNROAD AGGREGATES

Aggregate Geometric Property	Aggregate Size	
	¾"	
	1	2
Texture	176.4	213.4
Gradient Angularity	2841.0	2922.4
Sphericity	0.668	0.692
2D Form	7.405	7.596

DANNER ¾" CLASS D - MNROAD AGGREGATES

Aggregate Geometric Property	Aggregate Size	
	¾"	
	1	2
Texture	193.8	181.3
Gradient Angularity	2991.7	3014.8
Sphericity	0.722	0.657
2D Form	7.375	7.492

DANNER CRUSHED FINES - MNROAD AGGREGATES

Aggregate Geometric Property	Aggregate Size											
	#4		#8		#16		#30		#50		#100	
	1	2	1	2	1	2	1	2	1	2	1	2
Texture	159.3	186.3	NA		NA		NA		NA		NA	
Gradient Angularity	2563.8	2445.7	4078.1	3864.0	4142.4	4222.6	4460.4	3957.4	4214.0	4160.3	1899.8	2512.0
Sphericity	0.589	0.611	NA		NA		NA		NA		NA	
2D Form	8.714	8.794	8.665	8.602	8.577	8.938	8.819	8.257	8.820	8.580	7.4	8.352

OTTOPED SAND - MNROAD AGGREGATES

Aggregate Geometric Property	Aggregate Size											
	#4		#8		#16		#30		#50		#100	
	1	2	1	2	1	2	1	2	1	2	1	2
Texture	118.1	125.0	NA		NA		NA		NA		NA	
Gradient Angularity	1770.1	2077.5	2524.8	2563.4	2594.3	2695.7	3036.6	3085.7	3550.5	3256.0	2095.6	2429.2
Sphericity	0.700	0.701	NA		NA		NA		NA		NA	
2D Form	6.410	6.746	6.374	6.343	6.614	6.179	6.724	6.810	6.54	7.234	8.23	7.893

WACO AGGREGATES

Aggregate Geometric Property	Aggregate Size															
	½"		3/8"		#4		#8		#16		#30		#50		#100	
	1	2	1	2	1	2	1	2	1	2	1	2	1	2	1	2
Texture	127.2	128.1	139.5	143.3	136.3	140.0	NA		NA		NA		NA		NA	
Gradient Angularity	2809.9	2809.9	3034.9	2970.6	2908.6	3040.2	3468.0	3365.9	3442.0	3519.0	2961.6	3115.9	3441.8	3261.2	2123.7	1818.3
Sphericity	0.764	0.747	0.732	0.724	0.766	0.736	NA		NA		NA		NA		NA	
2D Form	6.417	6.663	7.058	7.318	7.741	7.226	7.871	7.812	7.577	7.463	7.142	6.970	7.567	7.562	7.652	7.058

ODESSA AGGREGATES

Aggregate Geometric Property	Aggregate Size											
	½"		3/8"		#4		#10		#40		#80	
	1	2	1	2	1	2	1	2	1	2	1	2
Texture	191.3	181.3	209.4	192.5	187.8	193.2	NA		NA		NA	
Gradient Angularity	2650.1	2848.0	2599.9	2719.5	3052.0	2936.5	3588.4	3452.5	3786.2	4046.5	1604.9	1638.6
Sphericity	0.778	0.806	0.772	0.771	0.714	0.710	NA		NA		NA	
2D Form	6.299	5.983	6.401	6.385	6.986	7.309	7.714	7.696	7.669	8.158	6.604	6.611

ATLANTA SANDSTONE AGGREGATES

Aggregate	Aggregate Size															
Geometric	½"		3/8"		#4		#8		#16		#30		#50		#100	
Property	1	2	1	2	1	2	1	2	1	2	1	2	1	2	1	2
Texture	121.3	120.3	140.8	128.8	153.4	171.7	NA		NA		NA		NA		NA	
Gradient Angularity	2800.8	2489.4	2768.7	2805.8	2200.1	2288.5	3925.2	3911.2	5119.0	4794.8	4611.5	4580.4	4942.6	4726.8	1947.1	2294.7
Sphericity	0.792	0.777	0.714	0.734	0.737	0.719	NA		NA		NA		NA		NA	
2D Form	6.084	6.226	6.726	7.037	7.553	7.691	8.208	8.084	9.049	9.113	9.057	8.933	10.042	10.088	6.910	7.519

ATLANTA QUARTZITE AGGREGATES

Aggregate Geometric Property	Aggregate Size															
	½"		3/8"		#4		#8		#16		#30		#50		#100	
	1	2	1	2	1	2	1	2	1	2	1	2	1	2	1	2
Texture	180.6	175.3	132.2	157.0	197.9	185.3	NA		NA		NA		NA		NA	
Gradient Angularity	2733.5	2919.4	3320.2	2935.4	3009.8	2926.4	3351.5	3508.5	3637.3	3786.6	3603.5	3698.8	3881.3	3899.0	1846.6	2080.9
Sphericity	0.767	0.725	0.689	0.714	0.627	0.615	NA		NA		NA		NA		NA	
2D Form	6.966	7.103	7.757	7.340	8.254	8.407	8.581	8.651	8.829	8.821	8.453	8.592	8.675	8.606	7.312	7.383

APPENDIX C

HMAC MIXTURE PROPERTY RESULTS

0 MONTHS AGED SPECIMEN RESULTS

Aging Condition (months)	HMAC Property	Replicate	HMAC Mixtures					
			MnROAD 01	MnROAD 02	Waco	Odessa	Atlanta Sandstone	Atlanta Quartzite
0	σ_t	1	235.04	264.9	678.65	362.66	637.4	837.2
		2	190.11	175.17	641.52	348.27	788.32	838.5
	E_t	1	327.67	456.54	957.48	733.93	1256.1	1544.2
		2	269.64	627.4	615.4	552.69	1699.3	1117.2
	m_t	1	0.3	0.32	0.52	0.44	0.4	0.46
		2	0.37	0.3	0.53	0.48	0.4	0.45
	E_c		417	813	915	530	1260	1338
			433	782	1108	916	1861	1462
	m_c		0.37	0.3	0.43	0.49	0.44	0.44
			0.44	0.33	0.44	0.43	0.41	0.44
	b	1	0.85	0.73	0.52	0.54	0.63	0.6
		2	0.88	0.76	0.52	0.60	0.66	0.62

3 MONTHS AGED SPECIMEN RESULTS

Aging Condition (months)	HMAC Property	Replicate	HMAC Mixtures					
			MnROAD 01	MnROAD 02	Waco	Odessa	Atlanta Sandstone	Atlanta Quartzite
3	σ_t	1	372	422	1033.73	756.04	937.4	1007
		2	369	451	1043.36	943.57	1062.79	1023.08
	E_t	1	NA	NA	1569.1	1577.1	2099.6	2120
		2			1629	1780.6	2145.1	2653.4
	m_t	1			0.3	0.25	0.28	0.29
		2			0.24	0.25	0.39	0.27
	E_c	1			1488	1432	1543	2265
		2			1781	1736	2917	2180
	m_c	1			0.37	0.3	0.25	0.3
		2			0.43	0.27	0.25	0.31
	b	1			0.83	0.81	1.17	1.12
		2			0.82	0.81	1.21	1.18

6 MONTHS AGED SPECIMEN RESULTS

Aging Condition (months)	HMAC Property	Replicate	HMAC Mixtures					
			MnROAD 01	MnROAD 02	Waco	Odessa	Atlanta Sandstone	Atlanta Quartzite
6	σ_t	1	475	629	1526.9	943.83	1555.22	1549.8
		2	470	648	1260.57	932.91	1411.94	1695.79
	E_t	1	NA	NA	2049.1	2025.6	3248.1	3326.2
		2			2015.5	2030.9	3003.4	3059.8
	m_t	1			0.24	0.23	0.25	0.23
		2			0.28	0.24	0.23	0.24
	E_c	1			3217	2066	3939	5105
		2			2898	2218	3251	3231
	m_c	1			0.31	0.24	0.28	0.23
		2			0.28	0.23	0.22	0.27
	b	1			1.58	1.64	1.36	1.32
		2			1.60	1.65	1.34	1.30

APPENDIX D

HMAC MIXTURE FATIGUE LIFE RESULTS

0 MONTHS AGED SPECIMEN RESULTS

ID	HMAC Mixtures					
	MnROAD 01	MnROAD 02	Waco	Odessa	Atlanta Sandstone	Atlanta Quartzite
N_{f1}	6.41E+07	2.55E+07	1.10E+07	8.39E+06	6.99E+06	6.48E+06
Ln N_{f1}	17.98	17.05	16.21	15.94	15.76	15.68
N_{f2}	6.41E+07	2.55E+07	1.10E+07	8.39E+06	6.99E+06	6.48E+06
Ln N_{f1}	17.98	17.05	16.21	15.94	15.76	15.68
N_{f3}	7.04E+07	9.66E+06	3.36E+07	1.52E+07	2.76E+06	1.66E+07
Ln N_{f1}	18.07	16.08	17.33	16.54	14.83	16.62
N_{f4}	7.04E+07	9.66E+06	3.36E+07	7.74E+06	2.76E+06	1.66E+07
Ln N_{f1}	18.07	16.08	17.33	15.86	14.83	16.62
N_{f5}	6.16E+07	1.11E+07	9.96E+06	7.74E+06	1.07E+07	6.50E+06
Ln N_{f1}	17.94	16.22	16.11	15.86	16.19	15.69
N_{f6}	6.16E+07	1.11E+07	9.90E+06	1.40E+07	1.07E+07	6.50E+06
Ln N_{f1}	17.94	16.22	16.11	16.45	16.19	15.69
N_{f7}	4.60E+07	4.23E+07	3.00E+07	1.40E+07	4.23E+06	1.66E+07
Ln N_{f1}	17.64	17.56	17.22	16.45	15.26	16.62
N_{f8}	4.60E+07	4.23E+07	3.00E+07	1.40E+07	4.23E+06	1.66E+07
Ln N_{f1}	17.64	17.56	17.22	16.45	15.26	16.62
Mean Ln Lab N_f	17.91	16.73	16.72	16.19	15.51	16.16
Mean Lab N_f	**5.98E+07**	**1.84E+07**	**1.82E+07**	**1.07E+07**	**5.44E+06**	**1.04E+07**
Stdev	0.17	0.65	0.60	0.31	0.55	0.50
COV (%)	**0.95**	**3.87**	**3.57**	**1.91**	**3.52**	**3.11**
Lower 95%CI (Ln Lab N_f)	17.76	16.19	16.22	15.93	15.05	15.74
Lower 95%CI (Lab N_f)	5.19E+07	1.07E+07	1.11E+07	8.29E+06	3.44E+06	6.82E+06
Upper 95%CI (Ln Lab N_f)	18.05	17.27	17.22	16.45	15.97	16.58
Upper 95%CI (Lab N_f)	6.89E+07	3.17E+07	3.00E+07	1.39E+07	8.58E+06	1.58E+07

3 MONTHS AGED SPECIMEN RESULTS

ID	HMAC Mixtures			
	Waco	**Odessa**	**Atlanta Sandstone**	**Atlanta Quartzite**
N_{f1}	7.76E+06	3.89E+06	2.02E+06	2.41E+06
Ln N_{f1}	15.86	15.17	14.52	14.70
N_{f2}	7.76E+06	3.89E+06	2.02E+06	2.41E+06
Ln N_{f1}	15.86	15.17	14.52	14.70
N_{f3}	6.54E+06	2.31E+06	2.23E+06	8.97E+05
Ln N_{f1}	15.69	14.65	14.62	13.71
N_{f4}	6.54E+06	2.31E+06	2.23E+06	8.97E+05
Ln N_{f1}	15.69	14.65	14.62	13.71
N_{f5}	7.90E+06	6.06E+06	2.59E+06	2.49E+06
Ln N_{f1}	15.88	15.62	14.77	14.73
N_{f6}	7.90E+06	6.06E+06	2.59E+06	2.49E+06
Ln N_{f1}	15.88	15.62	14.77	14.73
N_{f7}	6.66E+06	3.59E+06	2.87E+06	9.26E+05
Ln N_{f1}	15.71	15.09	14.87	13.74
N_{f8}	6.66E+06	3.59E+06	2.87E+06	9.26E+05
Ln N_{f1}	15.71	15.09	14.87	13.74
Mean Ln Lab N_f	15.79	15.13	14.69	14.22
Mean Lab N_f	**7.19E+06**	**3.74E+06**	**2.41E+06**	**1.49E+06**
Stdev	0.09	0.37	0.14	0.53
COV (%)	**0.58**	**2.42**	**0.98**	**3.72**
Lower 95%CI (Ln Lab N_f)	15.71	14.83	14.57	13.77
Lower 95%CI (Lab N_f)	6.66E+06	2.75E+06	2.13E+06	9.60E+05
Upper 95%CI (Ln Lab N_f)	15.86	15.44	14.81	14.66
Upper 95%CI (Lab N_f)	7.76E+06	5.08E+06	2.71E+06	2.33E+06

6 MONTH AGED SPECIMEN RESULTS

ID	HMAC Mixtures			
	Waco	**Odessa**	**Atlanta Sandstone**	**Atlanta Quartzite**
N_{f1}	4.47E+06	1.69E+06	6.07E+05	4.84E+05
Ln N_{f1}	15.31	14.34	13.32	13.09
N_{f2}	4.47E+06	1.69E+06	6.07E+05	4.84E+05
Ln N_{f1}	15.31	14.34	13.32	13.09
N_{f3}	5.69E+06	1.77E+06	7.17E+05	7.30E+05
Ln N_{f1}	15.55	14.39	13.48	13.50
N_{f4}	5.69E+06	1.77E+06	7.17E+05	7.30E+05
Ln N_{f1}	15.55	14.39	13.48	13.50
N_{f5}	3.05E+06	1.65E+06	5.00E+05	5.79E+05
Ln N_{f1}	14.93	14.32	13.12	13.27
N_{f6}	3.05E+06	1.65E+06	5.00E+05	5.79E+05
Ln N_{f1}	14.93	14.32	13.12	13.27
N_{f7}	3.88E+06	1.73E+06	5.91E+05	8.74E+05
Ln N_{f1}	15.17	14.36	13.29	13.68
N_{f8}	3.08E+06	1.73E+06	5.91E+05	8.74E+05
Ln N_{f1}	14.94	14.36	13.29	13.68
Mean Ln Lab N_f	15.21	14.35	13.30	13.39
Mean Lab N_f	**4.05E+06**	**1.71E+06**	**5.99E+05**	**6.50E+05**
Stdev	0.26	0.03	0.14	0.24
COV (%)	**1.74**	**0.19**	**1.03**	**1.79**
Lower 95%CI (Ln Lab N_f)	14.99	14.33	13.19	13.18
Lower 95%CI (Lab N_f)	3.24E+06	1.67E+06	5.34E+05	5.32E+05
Upper 95%CI (Ln Lab N_f)	15.43	14.38	13.42	13.59
Upper 95%CI (Lab N_f)	5.05E+06	1.75E+06	6.71E+05	7.95E+05

VITA

Edward Ofori-Abebresse was born in Accra, Ghana. He received his BSc. degree at the Kwame Nkrumah University of Science and Technology in Kumasi, Ghana in 2003. He began study toward his Master of Science degree in August 2004 at Texas A&M University. During this period he worked as a Graduate Research Assistant at the Texas Transportation Institute on a "Development of a Long Term Durability Specification for Modified Asphalt" project. He also worked as a Graduate Teaching Assistant for two undergraduate classes, Materials for Construction and Materials Engineering for Civil Engineers. Edward graduated in August 2006.

His permanent address is P.O. Box DS 1434, Dansoman, Accra, Ghana.